Effects of Compressibility Factor on Fluid Catalytic Cracking Unit Riser Hydrodynamics

Yakubu M. John, Raj Patel, Iqbal M. Mujtaba*

Chemical Engineering Division, School of Engineering, University of Bradford, Bradford, BD7 1DP, UK

* I.M.Mujtaba@bradford.ac.uk

Abstract

A detailed steady state FCC riser process model is simulated for the first time with different compressibility (Z) factor correlations using gPROMS software. A 4-lump kinetic model is used where gas oil cracks to form gasoline, coke and gases. The usual practice has been the assumption that the FCC riser gas phase is an ideal gas at every point under any condition (varying C/O ratio, riser diameter, operating temperature and pressure, etc.). This work found that the Z factor varies at every point across the riser height depending on riser operating pressure and temperature, diameter and C/O ratio. It also shows that the magnitude of deviation of a gas phase from ideal gas behaviour can be measured over the riser height. The Z factor correlation of Heidaryan et al., (2010a) is found to be suitable for predicting the Z factor distribution in the riser.

Keyword: FCC Riser; Modelling; Simulation; Compressibility Factor

1. Introduction

1.1 Background

The fluid catalytic cracking (FCC) operation is central to effective performance of a refinery. It converts refinery residues such as vacuum and atmospheric gas oil into the two important fuels; gasoline and diesel. The conversion is achieved in a pneumatic vessel called a riser. The pneumatic movement is caused by the riser-regenerator pressure gradient, which in turn determines the resident time of both gas oil and catalyst in the riser, and ultimately the yield of products. This process is effective if the riser hydrodynamics is efficient. Maintaining an efficient pressure gradient in the riser is a measure of good riser hydrodynamics that tends to improve product yield. A detailed model of the FCC can capture all the aspects of the unit that improves on the prediction of the performance of FCC risers (León-Becerril et al. 2004). As the feed meets the catalysts at the vaporization section, it vaporizes into the riser forming gas and catalyst phases that flows in a fluid-like manner to the top where it exits. The volume

of the products, which is the gas phase, increases as cracking of the feed proceeds bringing about changes in the density, molecular weight, temperature and pressure of the system along the riser height. All of the changes in those process variables depend on the type and nature of catalyst and feed. Due to this, properties like the crude oil American Petroleum Institute (API) gravity, density or specific gravity of feed and catalyst properties are specified in most FCC riser simulation. One of the process variables not always specified is the compressibility factor. Some authors (Ali et al. 1997; Han and Chung 2001a; Martignoni and de Lasa 2001; John et al. 2017b) have treated the gas compressibility of the vaporised fluid in the riser as unity. Others have assumed that the compressibility or Z factor can be a dimensionless value of one due to the fact that the riser operates at low pressure and high temperature (Ali et al. 1997; Fermoselli 2010), even though, at low pressure, 2 - 3% error is prevalent (Ahmed 2001). There is also an assumption that the density relationship of the gas phase model in the riser behaves as an ideal gas at any position in the riser even for a heavy oil feedstock (Martignoni and de Lasa 2001). Another researcher treated the gas phase in the riser as ideal gas with the assumption of constant enthalpy (Li et al. 2009). However, enthalpy is not constant in the riser (Han and Chung 2001b).

The Z-Factor is very significant in characterising the fluid flow of oil and gas in the upstream and downstream sector of the petroleum industries (Heidaryan et al. 2010a; Heidaryan et al. 2010b). The process that the fluid undergo describes whether it is compressible or non-compressible, and if there is a density change, as is possible in the riser, then the compressibility factor changes. Hence, treating the gaseous phase as an ideal gas in the case of changing density system will not be accurate. Also, as velocity increases, the density of the fluid varies and can be a compressible fluid (Balachandran 2007). Some process variables such as density (Lopes et al. 2012), viscosity and the void fraction would vary when change in mass (or moles) occur due to cracking reactions and when operating conditions such as temperature, mass flowrate and/or pressure (a function of gas compressibility) are altered. Since these changes in the operating conditions of the riser are taken into account when modelling risers (León-Becerril et al. 2004), the variation in the compressibility factor of the fluid needs to be considered too. One major operating determinant of the FCC unit is the catalyst circulation between the riser and regenerator, and it accomplishes two simple purposes: preserving the regenerated catalyst activity via regeneration and upholding the heat balance by the endothermic reactions in the riser and other forms of heat removal. The catalyst circulation in the FCC is possible by the overall pressure balance, which also has a

relationship with the gas compressibility factor. To get this pressure balance right, accurate conditions of the catalyst, feed and auxiliary equipment must synchronise with proper design of the FCC unit. In this work, the impact of the gas compressibility on the riser pressure, a major hydrodynamic parameter of the riser will be studied. This will identify the adequate compressibility factor at every point in the riser, which may give an accurate estimate of pressure drop and pressure balance in the riser and of the entire FCC unit. This will also determine the need for considering adequate gas compressibility factor to be used in plant design and not the outright assumption that the fluid phase is an ideal gas.

1.2 Motivation

One of the most unspecified quantities in the simulation, design and development of many process equipment for gas/solid handling is the compressibility factor because of the assumption that many gases behave like ideal gas. For the FCC riser reactor, the compressibility factor has always been assumed to be that of ideal gas. In reality, ideal gas is just an assumption and with all the assumptions made on how close the compressibility factor in the riser is to that of the ideal gas, there is no measured data in the literature to corroborate this. Of great interest in this work, is the accurate representation of gas Z-factor of the fluid in the riser. The accurate Z-factor will help to give an accurate estimate of hydrodynamic process variables such as pressure drop and pressure balance in the riser, and ensure effective process plant design.

1.3 Novel contributions of this study

This is the first study on compressibility factor of the riser where correlations are used through modelling as there is no such publication in the open literature. Some of the novel aspects of this paper are: (a) It is demonstrated that different Z factors produce different riser pressure and temperature responses, hence affect the product distribution of the riser (b) Once a C/O ratio is known, a correlation was obtained that can provide the pressure drop values across the riser height (c) A correlation is obtained for the varying Z factor as a function of C/O ratio. Once the C/O ratio of the riser is known, the change in Z can be obtained, which shows the extent in numerical terms how the real gas phase in the riser varies from the ideal gas phase (d) The Heidaryan et al., (2010a) Z factor correlation is found to be suitable for representing the Z factor across the riser. It affects the pressure regime in the riser.

2. Gas compressibility factor

The gas compressibility factor (Z-Factor) is a vital process variable in upstream and downstream calculations in petroleum industries (Heidaryan et al. 2010b), and its root equation is:

$$PV = ZnRT \tag{1}$$

The equation is suitable for real gases, and for ideal gas, Z is unity. An ideal gas does not exist in practice. Hence, an accurate gas compressibility factor needs to be used in some processes that handle gaseous phase flow or reactions. The compressibility factor is defined as the ratio of the actual volume of gas to the ideal volume of gas, meaning that it is a measure of the extent of deviation from perfect behaviour (Heidaryan et al. 2010b).

According to Fayazi et al., (2014), the Z-Factor can be easily obtained from experimental data, equation of state (EoS) and empirical correlations. Experimental methods are expensive and time consuming and there are numerous petroleum gases to account for (Ahmed 2001), whilst empirical correlations are found to be accurate and less complex than the EoS (Elsharkawy 2004). Having known the pseudo-reduced pressure and pseudo-reduced temperature of the fluid, empirical correlations offer a good estimate of the compressibility factor of the hydrocarbon gases (Fayazi et al. 2014). The model used in this work (Han and Chung 2001a; Han and Chung 2001b), captures the interactions of the pressures and temperatures in the vaporization and riser sections as functions of the pseudo-reduced pressures and temperatures. They obtain a correlation for the gas phase viscosities of the hydrocarbon lumps into pseudo-reduced viscosity and pseudo-critical viscosity using pseudo-reduced temperature in the range $\left(0.75 < T_{pr} < 3.0\right)$ and pseudo-reduced pressure in the range$\left(0.01 < P_{pr} < 0.2\right)$. Although, the pseudo-reduced temperature and pressure across the riser height for this simulation work lie outside the range that Han and Chung (2001a, b) used for the derivation of the correlation for the viscosities, the pseudo-reduced pressure from this work as shown in Figure 1 lies within the range of many correlations from the literature and presented in this work. This is to show the variations of the riser hydrodynamic variables with the compressibility factor, and since the pseudo-reduced pressures and pseudo-reduced temperatures vary along the riser, the compressibility factor may not be the same at all points in the riser.

Equations (50) and (51) in Table 2 are used in this work to obtain the pseudo-reduced temperature and pseudo-reduced pressure respectively and Figure 1 shows their variation

along the riser height. The pseudo-reduced pressure in this simulation is in the range $1.218066 \geq P_{pr} \geq 1.023427$ while the pseudo-reduced temperature is in the range $0.528144 \geq T_{pr} \geq 0.348992$. P_{pr} and T_{pr} may vary depending on the operating pressure and temperature of the riser and regenerator. This means that as the many process variables that influence the pressure and temperature of the FCC unit change during operation, P_{pr} and T_{pr} will also change. Consequently the Z factor, which is mostly dependent on the P_{pr} and T_{pr} will change too.

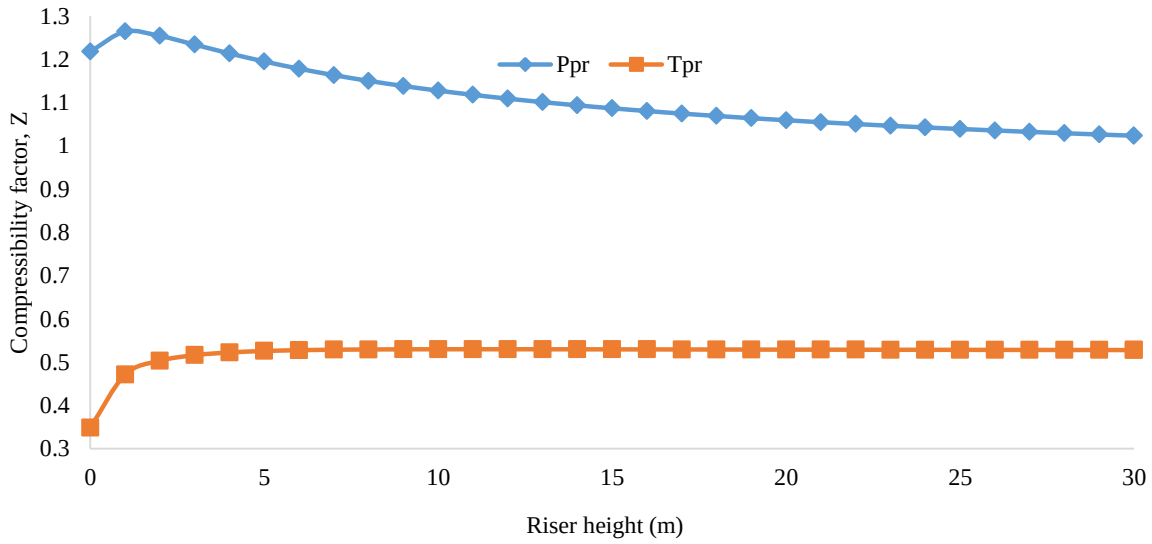

Figure 1: Pseudo-reduced pressure and temperature along riser height.

There are some common empirical correlations (Beggs and Brill 1973; Kumar 2004) which are not applicable to the pseudo-reduced temperatures equal or less than 0.92. Others that are used in this work accept T_{pr} above 0.92 (Heidaryan et al. 2010a; Sanjari and Lay 2012). To find a suitable correlation that predicts accurately or most closely the compressibility factor of the gas phase in the riser, a number of correlations were tested in this work. Each Z-factor correlation is inserted in the riser model and tested in this work. Important riser hydrodynamic variables such as inlet riser pressure and pressure drop will be compared for each Z-factor used. Results from the test will be compared with plant and literature data to determine which correlation estimates the riser Z-factor adequately. The T_{pr} in this simulation is out of the range of many of the correlations tested here, however, the P_{pr} is between

$1.218066 \geq P_{pr} \geq 1.023427$ which is consistent with all the ranges for all P_{pr} for all the correlations. The correlations are:

(a) Azizi et al. (2010) Zfactor:

Using Standing-Katz chart with 3038 points, Azizi et al. (2010) derived an empirical correlation for the compressibility factor over the range of $0.2 \leq P_{pr} \leq 11$ and $1.1 \leq T_{pr} \leq 2$, and is presented in Equation (2). The Zfactor is:

$$Z = A + \frac{B+C}{D+E} \tag{2}$$

The coefficients in Equation (2) are presented in Equations (3-7)

$$A = a\,T_{pr}^{2.16} + b\,P_{pr}^{1.028} + c\,P_{pr}^{1.58}T_{pr}^{-2.1} + d\,ln\,T_{pr}^{-0.5} \tag{3}$$

$$B = e + f\,T_{pr}^{2.4} + g\,P_{pr}^{1.56} + h\,P_{pr}^{0.124}T_{pr}^{3.033} \tag{4}$$

$$C = i\,ln\,T_{pr}^{-1.28} + j\,ln\,T_{pr}^{1.37} + k\,ln\left(P_{pr}\right) + l\,ln(P_{pr})^2 + m\,ln\left(P_{pr}\right)ln\left(T_{pr}\right) \tag{5}$$

$$D = 1 + n\,T_{pr}^{5.55} + o\,P_{pr}^{0.68}T_{pr}^{0.33} \tag{6}$$

$$E = p\,ln\,T_{pr}^{1.18} + q\,ln\,T_{pr}^{2.1} + r\,ln\left(P_{pr}\right) + s\,ln(P_{pr})^2 + t\,ln\left(P_{pr}\right)ln\left(T_{pr}\right) \tag{7}$$

The tuned coeffients for Equations (3-7) are presented in Appendix Table A.2.

(b) Bahadori et al. (2007) Z factor:

The Z-factor of Bahadori et al., (2007) is given in Equation (8) and its coefficients are presented in Equations (9-12) (Bahadori et al. 2007). The application range of this correlation is 0.2 < Ppr < 16 and 1.05 < Tpr < 2.4.

$$Z = a - bP_{pr} + cP_{pr}{}^2 + dP_{pr}{}^3 \tag{8}$$

$$a = Aa + BaT_{pr} + CaT_{pr}{}^2 + DaT_{pr}{}^3 \tag{9}$$

$$b = Ab + BbT_{pr} + CbT_{pr}{}^2 + DbT_{pr}{}^3 \tag{10}$$

$$c = Ac + BcT_{pr} + CcT_{pr}{}^2 + DcT_{pr}{}^3 \tag{11}$$

$$d = Ad + BdT_{pr} + CdT_{pr}{}^2 + DdT_{pr}{}^3 \tag{12}$$

The tuned coeffients for Equations (9-12) are presented in Appendix Table A.3.

(c) Heidaryan et al., (2010a) Z factor:

The Z-factor of Heidaryan et al., (2010a) is given in Equation (13) while the tuned coeffients are presented in Appendix Table A.4. The range for the pseudo-reduced pressures is $0.2 \leq P_{pr} \leq 3$. The range of the pseudo-reduced pressure in this work is consistent with that of Heidaryan et al., (2010a).

$$Z = \ln\left[\frac{A_1 + A_3\ln(P_{pr}) + \frac{A_5}{T_{pr}} + A_7(\ln P_{pr})^2 + \frac{A_9}{T_{pr}^2} + \frac{A_{11}}{T_{pr}}\ln(P_{pr})}{1 + A_2\ln(P_{pr}) + \frac{A_4}{T_{pr}} + A_6(\ln P_{pr})^2 + \frac{A_8}{T_{pr}^2} + \frac{A_{10}}{T_{pr}}\ln(P_{pr})}\right] \quad (13)$$

(d) Heidaryan et al., (2010b) Z factor:

The Z-factor of Heidaryan et al., (2010b) is given in Equation (14) while the tuned coeffients are presented in Appendix Table A.5. The range for the pseudo-reduced pressures and temperatures is $0.2 \leq P_{pr} \leq 15$ and $1.2 \leq T_{pr} \leq 3$ (Heidaryan et al. 2010b). The range of the pseudo-reduced pressure in this work is consistent with that of Heidaryan et al., (2010b).

$$Z = \frac{A_1 + A_2\ln(P_{pr}) + A_3(lnP_{pr})^2 + A_4(lnP_{pr})^3 + \frac{A_5}{T_{pr}} + \frac{A_6}{T_{pr}^2}}{1 + A_7\ln(P_{pr}) + A_8(lnP_{pr})^2 + \frac{A_9}{T_{pr}} + \frac{A_{10}}{T_{pr}^2}} \quad (14)$$

(e) Mahmoud (2014) Z factor:

The Z-factor correlation of Mahmoud (2014) is presented in Equation (15). It was based on 300 data points of measured compressibility factor and is a function of P_{pr} and T_{pr} only (Mahmoud 2014).

$$Z = \left(0.702e^{(-2.5T_{pr})}\right)P_{pr}^2 - \left(5.524e^{(-2.5T_{pr})}\right)P_{pr} + (0.044T_{pr}^2 + 1.15) \quad (15)$$

(f) Papay (1968) Z factor:

The Z-factor correlation of Papay presented in 1968 is described by Equation (16) (Li et al. 2014).

$$Z = 1 - \frac{P_{pr}}{T_{pr}}\left[0.3648758 - 0.04188423\left(\frac{P_{pr}}{T_{pr}}\right)\right] \quad (16)$$

(g) Sanjari and Lay (2012) Z factor:

The Z-factor model developed by Sanjari and Lay (2012) was derived from 5844 experimental data of compressibility factors for a range of 0.01 ≤ Ppr ≤15 and 1 ≤Tpr ≤ 3, and correlation is presented in Equation (17), while its tuned coefficients are presented in Appendix Table A.6.

$$Z = 1 + A_1 P_{pr} + A_2 (P_{pr})^2 + \frac{A_3 P_{pr}^{A_4}}{T_{pr}^{A_5}} + \frac{A_6 P_{pr}^{(A_4+1)}}{T_{pr}^{A_7}} + \frac{A_8 P_{pr}^{(A_4+2)}}{T_{pr}^{(A_7+1)}} \quad (17)$$

(f) Shokir et al., (2012) Z factor:

The Shokir et al., (2012) Z-factor is presented in Equation (18), while its various terms are presented in Equations (19-23)(Shokir et al. 2012).

$$Z = A + B + C + D + E \quad (18)$$

$$A = 2.679562 \frac{(2T_{pr} - P_{pr} - 1)}{[(P_{pr}^2 + T_{pr}^3)/P_{pr}]} \quad (19)$$

$$B = -7.686825 \left[\frac{(P_{pr}T_{pr} + P_{pr}^2)}{[(P_{pr}T_{pr} + 2T_{pr}^2 + T_{pr}^3)]}\right] \quad (20)$$

$$C = -0.000624 (P_{pr}{T_{pr}}^2 - T_{pr}P_{pr}^2 + T_{pr}P_{pr}^3 + 2P_{pr}T_{pr} - 2P_{pr}^2 + 2{P_{pr}}^3) \quad (21)$$

$$D = 3.067747 \frac{(T_{pr} - P_{pr})}{[(P_{pr}^2 + T_{pr} + P_{pr})]} \quad (22)$$

$$E = \frac{0.068059}{P_{pr}T_{pr}} + 0.139489{T_{pr}}^2 - 0.081873P_{pr}^2 - \left[\frac{0.041098T_{pr}}{P_{pr}}\right] + \left[\frac{8.152325P_{pr}}{T_{pr}}\right] - 1.63028P_{pr} + 0.24287T_{pr} - 2.64988 \quad (23)$$

3. Process Modelling

This section presents the riser description, the model assumptions, the model equations and the parameters used for the model simulation.

3.1 The Riser

The riser in a FCC unit is a vertical cylinder as shown in Figure 2 and modelled here as a one-dimensional plug flow reactor without axial and radial dispersion. The riser is 30 m in height and 1.1 m in diameter. Other parameters used in this simulation of the riser are found in the Appendix Table A.7.

A simulation is a virtual representation, therefore some assumptions are unavoidable, and hence, the momentum, mass and energy balance equations for the catalyst and gaseous

phases are obtained under the following assumptions (Han and Chung 2001a; John et al. 2017a):

1. The gas oil vaporizes instantly when it comes in contact with the regenerated catalyst.
2. The vaporized content of the riser moves upwards in thermal equilibrium with the catalyst phase.
3. It is considered that the riser is operated adiabatically (Ali et al. 1997).
4. The riser is a reactor where the cracking reactions takes place and only on the catalyst surface.
5. The reaction is fast and the riser is considered a steady state model.
6. The vaporization section is considered in this simulation.

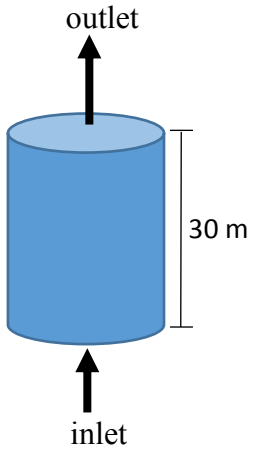

Figure 2: The Riser in a FCC.

At the vaporization section, the regenerated catalyst from the regenerator meets the feed, which vaporizes instantaneously and flows pneumatically upwards into the riser. This contact causes a cracking reaction on the surface of the catalyst to form valuable fuels such as gasoline, gases and coke, based on the four-lumped model. The four-lumped kinetic model obtained from the literature (Lee et al. 1989) was used in this study and is shown in Figure 3. It shows gas oil cracking into gasoline, gases and coke.

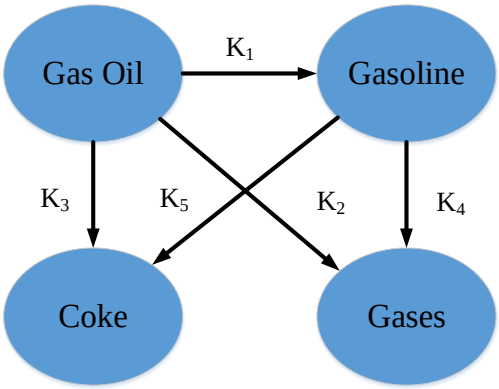

Figure 3**:** Four-lumped model of gas oil cracking reactions (Lee et al. 1989).

It is difficult to have a kinetic model which adequately represents all chemical reactions involved in the cracking of gas oil (Mehran Heydari 2010; Liu 2015). Therefore, many authors classified the reactant and products into valuable lumps. The kinetic model presented in Figure 3 is the cracking reaction that breaks down gas oil into gases, coke and gasoline. The four-lumped model is used by most authors (Han and Chung 2001a; John et al. 2016; John et al. 2017a; John et al. 2017b) and widely acceptable due to the fact that it considers the useful riser products (Cristina 2015). The heat necessary for the riser endothermic cracking reaction is sourced from catalyst regeneration. Therefore, the accurate amount of coke formed due to catalyst deactivation needs to be determined to aid heat integration and reactor temperature control in the regenerator. This is one of the advantages of the four-lump model (Han and Chung 2001a).

The following constants K_1, K_2, K_3, K_4 and K_5 shown in Figure 3, are the overall rate constants for the riser cracking reactions whose parameters are presented in Table A.3 in the Appendix. The cracking of gas oil to form gasoline, gases and coke is considered a second order reaction as shown in Table 1, and the cracking of gasoline to form gases and coke is considered a first order reaction.

Table 1: Four-lump gas oil cracking reaction (Han and Chung 2001b)

Four-lump	order of reaction
Gas oil – Gasoline	2
Gas oil –C_1-C_4 gases	2
Gas oil- Coke	2
Gasoline–C_1-C_4 gases	1

3.2 Model Equations

The model equations used in this work with their parameters and feed conditions were taken from the literature (Han and Chung 2001a; Han and Chung 2001b; John et al. 2017a). A 4-lumped kinetic model which cracks gas oil into gasoline, gases and coke as explained earlier is used. The 4-lumped kinetic model is commonly used when gasoline and coke are the most important products of the riser, unlike the 3-lumped model, which has no coke as a lump. The coke is burnt to generate the endothermic heat required for the cracking reactions in the riser, hence the usefulness of the 4-lumped model. Other lumped models including the 10-lumped model are suitable in the event that the subdivisions of fractional yields are required (Han and Chung 2001a). Some lumped kinetic models produce coke as well but sometimes the interest is more than just gasoline and coke.

Figure 2 shows a diagram of the riser and it is modelled as a one-dimensional cylindrical reactor based on momentum, mass and energy balance equations. The one-dimensional homogeneous plug-flow model is not complicated and it is able to take up to 30,000 reactions incorporating about 3000 different reacting species. Unlike the CFD and the multi-dimensional flow models where chemical reactions are necessarily small (He et al. 2015). Although multi-dimensional models capture the very comprehensive geometric views of the hydrodynamics and heat transfer in a FCC riser, it was established that the overall performance of the riser can be predicted using this simple one-dimensional total mass, energy, and chemical species balances (Theologos and Markatos 1993).

Equations (24-66) presented in Table 2 and those in the Appendix (Equations (A.1 – A.34)), which are mostly correlations were all used in this simulation. All equations are taken from the literature (Han and Chung 2001a; Han and Chung 2001b; John et al. 2017a)

Table 2: Equations and descriptions

Equations	description	number
$\frac{dT_c}{dx} = \frac{\Omega h_p A_p}{F_c C_{pc}} (T_g - T_c)$	temperature of catalyst along the riser height	(24)
$\frac{dT_g}{dx} = \frac{\Omega}{F_g C_{pg}} \left[h_p A_p (T_c - T_g) + \rho_c \varepsilon_c Q_{react}\right]$	temperature of gas phase along the riser height	(25)
$\frac{d_{y_{go}}}{dx} = \frac{\rho_c \varepsilon_c \Omega}{F_g} R_{go}$	gas oil fractional yield along the riser height	(26)
$\frac{d_{y_{gl}}}{dx} = \frac{\rho_c \varepsilon_c \Omega}{F_g} R_{gl}$	gasoline fractional yield along the riser height	(27)
$\frac{d_{y_{gs}}}{dx} = \frac{\rho_c \varepsilon_c \Omega}{F_g} R_{gs}$	light gas fractional yield along the riser height	(28)
$\frac{d_{y_{ck}}}{dx} = \frac{\rho_c \varepsilon_c \Omega}{F_g} R_{ck}$	coke fractional yield along the riser height	(29)
$R_{go} = -(K_1 + K_2 + K_3) \emptyset_c {y_{go}}^2$	rates of reaction for gas oil R_{go}	(30)
$R_{gl} = (K_1 {y_{go}}^2 - K_4 y_{gl} - K_5 y_{gl}) \emptyset_c$	rates of reaction for gasoline R_{gl}	(31)
$R_{gs} = (K_2 {y_{go}}^2 - K_4 y_{gl}) \emptyset_c$	rates of reaction for light gas R_{gs}	(32)
$R_{ck} = (K_3 {y_{go}}^2 - K_5 y_{gl}) \emptyset_c$	rates of reaction for coke R_{ck}	(33)
$K_1 = k_{10} \exp\left(\frac{-E_1}{RT_g}\right)$	overall rate constants for cracking gas oil to gasoline	(34)

$K_2 = k_{20} \exp\left(\frac{-E_2}{RT_g}\right)$	overall rate constants for cracking gas oil to gases	(35)
$K_3 = k_{30} \exp\left(\frac{-E_3}{RT_g}\right)$	overall rate constants for cracking gas oil to coke	(36)
$K_4 = k_{40} \exp\left(\frac{-E_4}{RT_g}\right)$	overall rate constants for cracking gasoline to gases	(37)
$K_5 = K_{50} \exp\left(\frac{-E_5}{RT_g}\right)$	overall rate constants for cracking gasoline to coke	(38)
$Q_{react} = -\left(\Delta H_1 K_1 {y_{go}}^2 + \Delta H_2 K_2 {y_{go}}^2 + \Delta H_3 K_3 {y_{go}}^2 + \Delta H_4 K_4 y_{gl} + \Delta H_5 K_5 y_{gl}\right)\emptyset_c$	Q_{react} is the rate of heat generation or heat removal by reaction	(39)
$\varepsilon_g = 1 - \varepsilon_c$	gas volume fraction, ε_g, and catalyst volume fraction, ε_c,	(40)
$\varepsilon_c = \frac{F_c}{v_c \rho_c \Omega}$	gas volume fraction, ε_g, and catalyst volume fraction, ε_c,	(41)
$\Omega = \frac{\pi D^2}{4}$	cross sectional area of the riser,	(42)
$A_{ptc} = \frac{6}{0.72 d_c} * (1 - \varepsilon_g)$	The effective interface heat transfer area per unit volume between the catalyst and gas phases	(43)
$\emptyset_c = \exp(-\alpha_c C_{ck})$	catalyst deactivation	(44)
$\alpha_c = \alpha_{c0} \exp\left(\frac{-E_c}{RT_g}\right)(R_{AN})^{\alpha_{c*}}$	catalyst deactivation coefficient	(45)
$C_{ck} = C_{ckCL1} + \frac{F_g y_{ck}}{F_c}$	coke on catalyst	(46)

$\rho_g = \frac{F_g}{\varepsilon_g v_g \Omega}$	density of the gas phase	(47)
$P_{RS} = \rho_g \frac{RT_g}{M_{wg}}$	riser pressure	(48)
$C/O \text{ ratio} = \frac{F_c}{F_g}$	catalyst-to-oil ratio	(49)
$T_{pr} = \frac{T_g}{T_{pc}}$	pseudo-reduced temperature in the riser	(50)
$P_{pr} = \frac{P_{RS}}{P_{pc}}$	pseudo-reduced pressure in the riser	(51)
$\frac{dv_c}{dx} = -\left(G_c \frac{\Omega}{F_c}\frac{d\varepsilon_c}{dx} - \frac{C_f(v_g - v_c)\Omega}{F_c} + \frac{2f_{rc}v_c}{D} + \frac{g}{v_c}\right)$	catalyst and gas velocity distribution across the riser	(52)
$\frac{dv_g}{dx} = -\left(\frac{\Omega}{F_g}\frac{dP_{RS}}{dx} - \frac{C_f(v_c - v_g)}{F_g} + \frac{2f_{rg}v_g}{D} + \frac{g}{v_g}\right)$	catalyst and gas velocity distribution across the riser	(53)
$G_c = 10^{(-8.76\varepsilon_g + 5.43)}$	stress modulus of the catalyst (Tsuo and Gidaspow 1990)	(54)
$T_{cFS} = T_{cCL1} - \frac{F_{lg}}{F_{cCL1}C_{pc}}\left[C_{plg}(T_{gFS} - T_{lg}) + \frac{F_{ds}C_{pds}}{F_{lg}}(T_{gFS} - T_{ds}) + \Delta H_{vlg}\right]$	catalyst temperature at the vaporization section	(55)
$T_{gFS} = \frac{B_{lg}}{A_{lg} - log(P_{FS}y_{goFS})} - C_{lg}$	gas phase temperature at the vaporization section	(56)
$P_{FS} = P_{RT} + \Delta P_{RS}$	pressure at the vaporization	(57)

$y_{goFS} = \frac{\mathrm{F_{lg}}}{\mathrm{F_{lg}} + \mathrm{F_{ds}}}$	weight fraction of feed (gas oil) at the vaporization section	(58)
$v_{gFS} = \frac{\mathrm{F_{lg}} + \mathrm{F_{ds}}}{\rho_{\mathrm{gFS}}(1 - \varepsilon_{cCL1})\Omega_{FS}}$	velocity of gas phase at the vaporization section	(59)
$v_{cFS} = \frac{\mathrm{F_{cCL1}}}{\rho_{\mathrm{c}}\, \varepsilon_{cCL1}\Omega_{FS}}$	velocity of entrained catalyst at the vaporization section	(60)
$\rho_{gFS} = \frac{\mathrm{P_{FS}M_{wgFS}}}{\mathrm{RT_{gFS}Z_{gFS}}}$	gas oil density at the vaporization section	(61)
$v_{cFS}^{(0)} = v_{cFS}$	catalyst phase velocity	(62)
$v_{gFS}^{(0)} = v_{gFS}$	gas phase velocity	(63)
$\mathrm{F_{cRS}} = \mathrm{F_{cCL1}}$	catalyst mass flowrate	(64)
$\mathrm{F_{gRS}} = \mathrm{F_{lg}} + \mathrm{F_{ds}}$	gas phase mass flowrate	(65)
$\Delta H_{vlg} = 0.3843T_{MABP} + 1.0878 * 10^3\, exp\left(\frac{-M_{wm}}{100}\right) - 98.153$	heat of vaporization of gas oil	(66)

Equations 24 and 25 are derived from the energy balance of the riser showing the temperature of catalyst and gas phases. Equations (26 - 29) were obtained from the material balance for the reaction showing the four lumps; gas oil, gasoline, light gas and coke respectively. The respective overall rates of reaction for gas oil R_{go}, gasoline R_{gl}, light gas R_{gs}, and coke R_{ck}, are given in Equations (30-33). Each overall rate of reaction is function of an overall rate constant which is described by the Arrhenius equation given in Equations (34-38). The overall rate constants K_i, of reaction path i = 1 to 5 are also a function of their corresponding frequency factors k_{i0} .

During the cracking reaction, heat generated from the regenerator is utilized in the riser and the rate of heat generation or heat removal by reaction Q_{react} is estimated by Equation (39). The gas volume fraction, ε_g, and catalyst volume fraction, ε_c, are obtained from Equations (40) and (41) respectively. They give a hydrodynamic constraint such that the summation of the volume fractions add up to unity. The riser pressure is given by Equation (48) and is obtained from the simple ideal gas relationship with Z as compressibility factor. The simulation model incorporates the momentum balance equations which gives catalyst and gas velocity distribution across the riser as shown in Equations (52 and 53).

At the vaporization section, the system is modelled as a mixed stream of hot catalyst and feed. The catalyst temperature is obtained from the energy balance while the gas phase temperature is obtained using the Antoine equation. The catalyst and gas phase temperatures at the vaporization section are given by Equations (55) and (56) respectively. Boundary conditions are set for the riser entrance; the velocitiy of catalyst and gas phase at the vaporization section equals the entrance velocities to the riser. These velocities are presented in Equations (62 and 63).

3.3 Model Solution

The equations generated for the riser are a set of nonlinear equations and gPROMS is used to solve them. gPROMS is a general process modelling system for simulation, optimisation and control (both steady state and dynamic) of highly complex processes such as the FCC unit. It is one of the available equation oriented software suitable for the type of equations developed for the riser of FCC unit. All solvers have been designed specifically for large-scale systems and there are no limits regarding problem size other than those imposed by available machine memory (Mujtaba 2012). In spite of the robustness of gPROMS and to the best of the

authors' knowledge, there is no mention in the literature of the use of the software to solve the models of the FCC unit. This is the first attempt and gPROMS has proved to be a reliable software. The riser model is constructed in the model section and the parameters are specified in the process section of the gPROMS 4.0.1 software. The gPROMS software is capable of analysing the set of equations to determine the stiffness of the system and calls on the appropriate solvers. In this case solvers capable of solving the nonlinear system of equations of the riser model.

4. Results and Discussions

Here the simulation results are presented and compared with results from Han and Chung (2001a, b). The simulation results are also compared with plant data. Han and Chung (2001a, b) validated their simulation results against plant data, which means comparing this simulation results with theirs is validation in a sense. Simulation results from this study are also validated against plant data. Another reason for presenting the simulation results is to demonstrate the capability of gPROMS in solving complex nonlinear DAEs, again, by validating the results against those predicted by the same model but using different solution software as DSim-FCC (Han and Chung 2001b).

4.1 Simulation

Gas oil meets the catalyst at the vaporization section and vaporizes into the riser as it begins to crack to form cracked lumps; gasoline, gases and coke. In this study, the cracking reaction is set to take place at gas oil inlet temperature of 535 K and catalyst inlet temperature of 1006.4 K. In addition, the mass flow rate of catalyst and gas oil is 300 kg/s and 49.3 kg/s respectively, which means a catalyst-oil-ratio (C/O) ratio of 6.085 as in the case of Han and Chung (2001a, b). The profiles of the products are shown in Figure 4.

The gas oil comes into the riser at 0.9686 (kg lump/kg feed) fraction and its unconverted fraction at the exit of the riser is 0.3045 (kg lump/kg feed) corresponding to 29.56% unconverted. This shows that 70.44% of gas oil feed was consumed and 60% of the fraction was consumed in the first 18 m of the riser. In Han and Chung (2001b) the fraction of gas oil at the exit of the riser is 0.2735 (kg lump/kg feed) which corresponds to 69.51% of gas oil consumed. This difference can be caused by the difference in the inlet temperature of catalyst to the riser, because increase in catalyst temperature can increase conversion (John et al. 2017b). This would further explain the reason for some differences for the other lumps:

gasoline, gases and coke. The profile of gasoline rose from 0 (kg lump/kg feed) at the inlet of the riser to its maximum yield of 0.4998 (kg lump/kg feed) at the exit of the riser. The yield compares well with the value of about 0.5085 (kg lump/kg feed) which is 50.85 wt% obtained by Han and Chung (2001b). The coke concentration also rose from 0 (kg lump/kg feed) at the inlet to 0.038 (kg lump/kg feed) at the exit of the riser while that reported by Han and Chung (2001b) is 0.0472 (kg lump/kg feed). The yield of the gases rose from 0 (kg lump/kg feed) at the inlet of the riser to a maximum of 0.1262 (kg lump/kg feed) at the exit while that of Han and Chung (2001b) is 0.141 (kg lump/kg feed). The profile of gases and coke in this work compares qualitatively well with the validated results obtained by Han and Chung (2001b) where the same model was adopted. The difference in the quantity of gasoline produced in this simulation and that of Han and Chung (2001b) is 1.7% and in the case of the lump, gases, an increase of 10.49% yield was obtained due to higher catalyst inlet temperature as earlier stated.

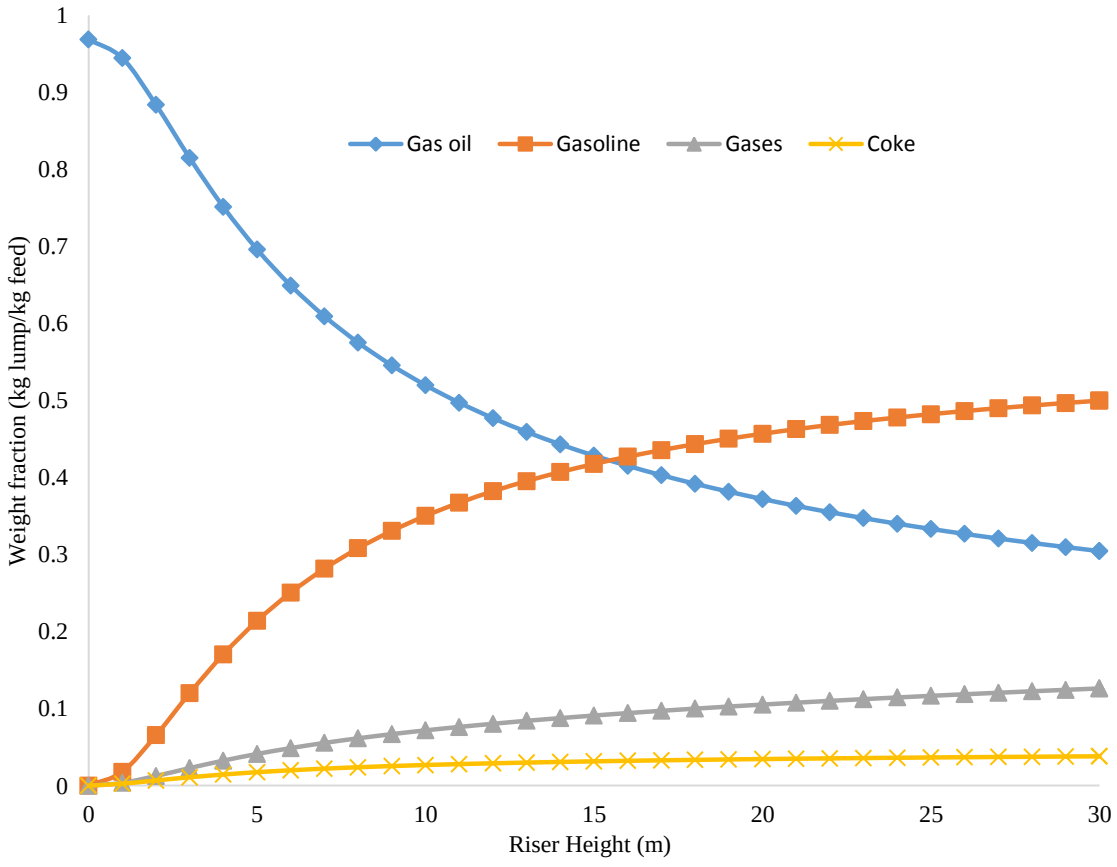

Figure 4: Lumps profiles along the riser

Figure 5 shows the temperature profiles of the gas and catalyst phases as a function of riser height for this simulation. The inlet temperature of the catalyst-phase, which comes from the

vaporization section as 1006.4 K drastically decreases to a minimum in the first 6 m and continue to decrease until it eventually levels out to the riser exit. The inlet temperature of the gas phase, which comes from the vaporization section at 535 K also rises to a peak in the first 11 m of the riser and levels out for the remaining portion of the riser. Both profiles, with a difference of 483.5 K at the riser inlet, only have a difference of 1.6 K at the exit of the riser. The difference in these temperatures provides the heat of reaction necessary for completion of the reaction. The temperature profiles obtained in this work are similar to those obtained in many literatures (Ali et al. 1997; Han and Chung 2001b; Souza et al. 2006; John et al. 2017b).

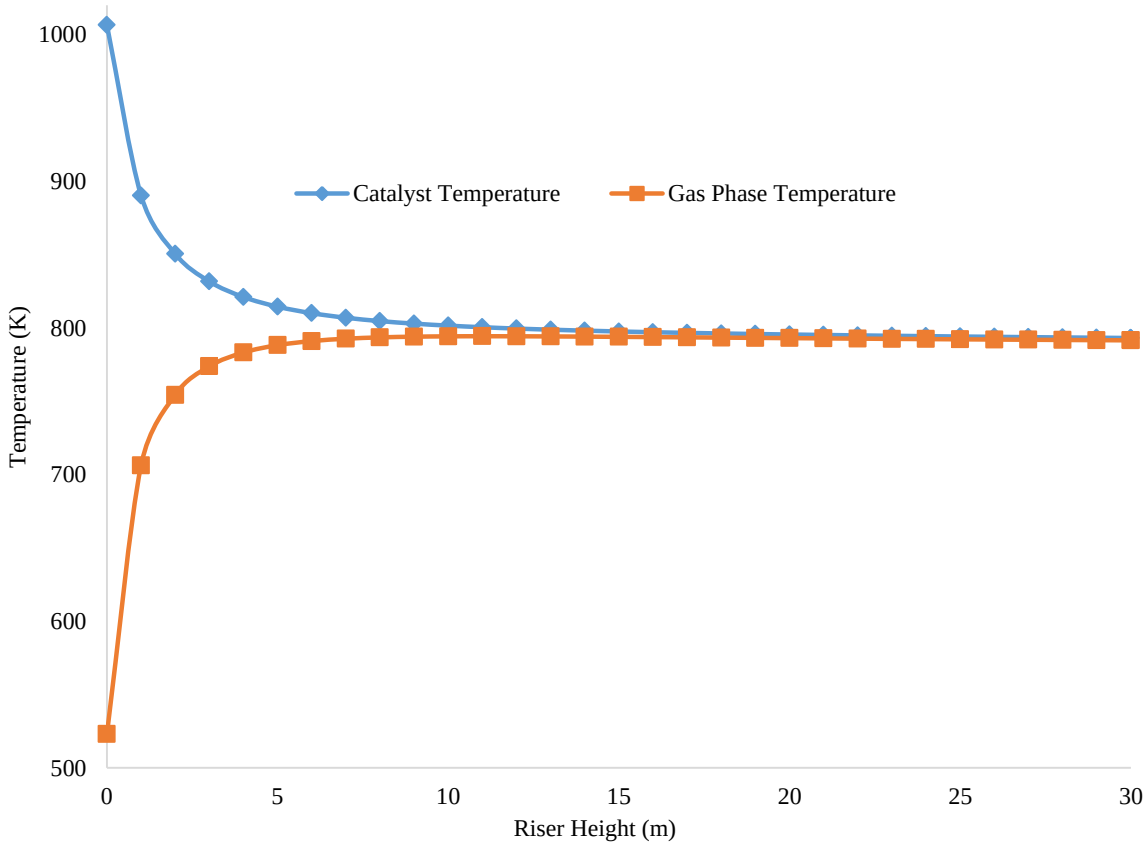

Figure 5: Temperature profile along the riser

The velocity profiles of the gas and catalyst phases along the riser height are shown in Figure 6. The catalyst and gas velocities emanated from the vaporization section of the riser unit and rises relatively sharply from about 10.32 m/s at the riser inlet for the gas to about 33.17 m/s at the exit of the riser, and likewise 11 m/s for the catalyst at the inlet to 33.41 m/s at the exit. During the cracking reactions, the slip velocity between the two phases is maintained within

0.675 m/s at the inlet of the riser to 0.246 m/s at the exit of the reactor. The average is comparable to the slip velocity of 0.25 m/s obtained by Han and Chung (2001b). The velocity profiles of the phases of gas and catalyst show that velocity is not constant along the height of the riser during cracking and it is due to the molar expansion of gases formed as the catalyst moves upward.

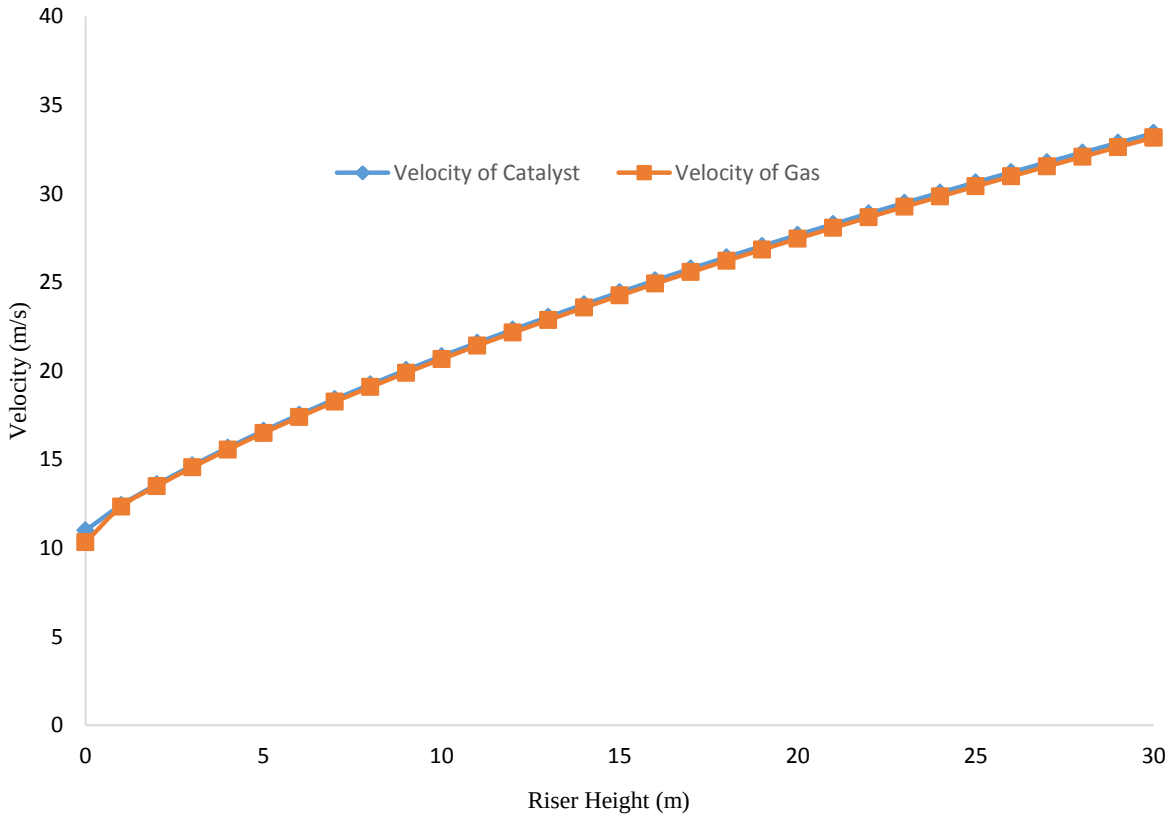

Figure 6: Velocity profile of gas and solid phases

Figure 7 shows the pressure profile in the riser, which decreases practically linearly from 242.32 kPa at the inlet of the riser coming from the vaporization section to 203.59 kPa at the exit of the riser. However, in the first 1 m of the riser the pressure rose sharply to 251.49 kPa, mainly due to the vigorous mixing because of the instantaneous vaporization in the vaporization section before it steadily decreases towards the outlet of the riser. The total pressure drop is 38.73 kPa for this simulation against 16 kPa, obtained by Han and Chung (2001b). This pressure drop of 38.73 kPa is quite big but can compare closely with operation log data obtained from the Kaduna refinery: 0.28 kg/cm^2 (27.46 kPa) in February 2012; 0.23 kg/cm^2 (22.56 kPa) in April 2014; 0.25 kg/cm^2 (24.52 kPa) in September 2014 and was allowed to have up to 0.31 kg/cm^2 (30.4 kPa). Therefore, the pressure drop in practice could

be greater than 16 kPa obtained by Han and Chung (2001b). Another reason for this pressure drop difference is due to the fact that this simulation only considered part of the riser section of the FCC unit; the riser reactor and the vaporization section. The riser pressure is also influenced by the pressure of the disengaging-stripping section and the pressure of the regenerator section which were all considered in the Han and Chung (2001a, b) simulation but not considered in this simulation. . However, the velocities and pressure profiles are qualitatively similar with results obtained by Han and Chung (2001b).

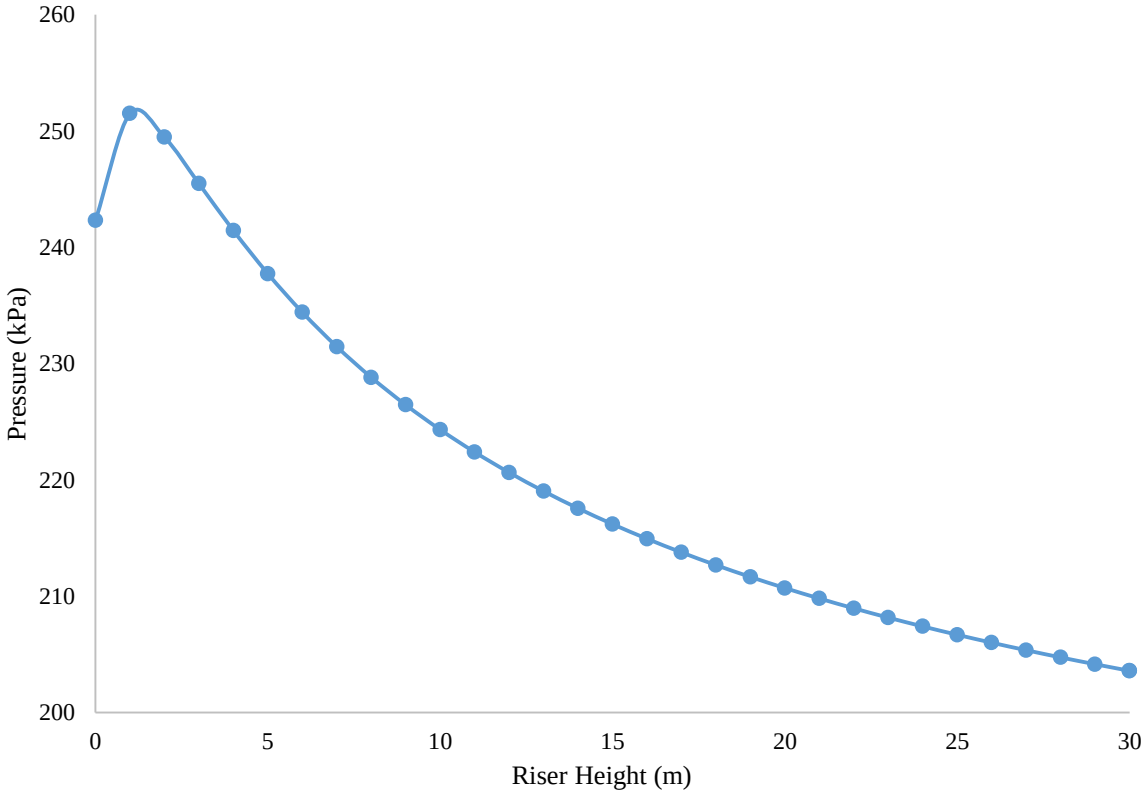

Figure 7: Pressure profile along the riser

In order to determine the accuracy of this work and to validate the capability of this gPROMS model, results from validated work of Han and Chung (2001a, b) shown in column B of Table 3, and Kaduna refinery operational data shown in column C, are used to compare with the results of this simulation work. The catalyst-to-oil ratio (C/O) in this simulation is 6.085, while for the data obtained from Kaduna refinery, the C/O ratio is 7.0. This means that the Kaduna refinery plant data may not be an exact pivot for comparison with this simulation results since the yields from a riser are functions of the feed quality, catalyst type, reaction temperature, catalyst to oil ratio and many other operational variables. However, the

deviation may not be too large and small marginal error limits can still be acceptable. Hence, Kaduna refinery data can still be used for validation of this simulation along with the simulation results of Han and Chung (2001a, b) whose plant operational conditions and riser configuration are the same as those used in this simulation.

Table 3: Comparison of this riser simulation output results in column A, with Han and Chung (2001a, b) simulation in column B, and plant data from Kaduna refinery in column C (Chiyoda 1980).

Parameter	Input	Riser output				
		A (This Simulation)	B (Han and Chung (2001a, b)	C (Kaduna Refinery)	% Deviation	
					A with B	A with C
Gas oil Temperature (K)	535	791.5	793.5	800.0	-0.25	-1.07
Catalyst Temperature (K)	1006	793.1	796.1		-0.38	
Gas oil mass flowrate (kg/s)	49.3	49.3	49.3			
Catalyst mass flowrate (kg/s)	300	300	300			
Gas oil mass fraction	0.969	0.3045	0.2735	0.236	10.18	22.49
Gasoline mass fraction	0	0.4997	0.5085	0.515	-1.76	-3.06
Gases mass fraction	0	0.1261	0.1410	0.198	-11.82	-57.01
Coke mass fraction	0	0.0381	0.0427	0.051	-12.07	-33.86

Han and Chung (2001a, b) simulation results had been validated against plant and literature data, which makes it suitable to be referenced here. From Table 3, the deviation (column A with B) between the results of this simulation (column A) and the Han and Chung (2001a, b) (column B) are within a marginal error of less than 4 %, except for mass fractions of gas oil and coke. The mass fraction of gasoline and temperatures are the most important parameters to compare here and seemed to conform adequately. Hence, it shows that gPROMS is accurate in predicting the results obtained by Han and Chung (2001a, b) and can be recommended for the simulation of the FCC unit as a whole. The deviation between the results of this simulation (column A) and the plant data (column C) for key components like temperatures and gasoline fraction is also within a marginal error limit of 4%. Others are quite wide mainly due to differences in the feed quality, catalyst type, reaction temperature, C/O ratio and other operational variables that differ in the two sets of results. Many literatures

however show that the profiles of the yields of gas oil, gasoline, gases, coke and temperatures obtained from this gPROMS simulation are qualitatively consistent (Ali and Rohani 1997; Han and Chung 2001b; Cristina 2015; John et al. 2017b).

4.2 Z Factor analysis

In trying to investigate the effect of the compressibility factor on the riser, various correlations were included in the riser model for the first time. The simulation is run under the same condition of C/O ratio of 6.085. Figure 8 shows the profiles of Z factor along the riser height. Z factor correlation models of Sanjari and Lay (2012) and Shokir et al., (2012) produced negative Z factors along the riser height because of the range of P_{pr} and T_{pr} of this simulation. Hence, their profiles are not included in Figure 8. Each Z factor varies along the riser height because of the dependency of some variables such as temperature, pressure, density as well as viscosity, heat of reaction and molar change in composition. At any point for each Z factor model, the Z value is not the same. The Z factor for the assumed ideal gas, being Z = 1, remained constant throughout the riser height while from the Z factors shown in Figure 8, it is clear that Z factor varies along the riser.

From Figure 8, it is clear that not all the Z factor equations can adequately represent the true values of Z factor in the riser. Many of the simulation results are far away from the ideal gas prediction as seen in Figure 8, with only the Z factor correlation of Heidaryan et al, (2010a) coming close. However, this does not that the Z factor correlation of Heidaryan et al, (2010a) is the true representation of the Z factor in the riser, there is need to investigate further how it relates to other process variables in the riser.. Many other factors may need to be considered. Factors such as the yield of gasoline and conversion of gas oil for each Z factor correlation, the temperature profiles of the solid and gaseous phases, the pressure profile and pressure drop along the column, the viscosity, which is dependent on P_{pr} and T_{pr} , the C/O ratio and riser diameter.

Figure 9 shows the profiles of viscosity of the gas phase along the riser height. Fluid catalytic cracking breaks down larger hydrocarbon molecules, which due to higher molecular weight have higher viscosity, but when broken-down, the lower molecular weight hydrocarbons tends to have lower viscosity. Hence, the viscosity of the gas oil should be higher at the inlet of the riser and when cracking starts, lower molecular weight hydrocarbons such as gasoline and gases forms the gaseous phase in the riser and the viscosity begins to decrease as seen in Figure 9. Although it shows that for ideal gas, the viscosity drops along the riser, one should

bear in mind that viscosity is a function of temperature which varies along the riser. From Figure 9, it can be seen that every Z factor represents a different viscosity profile, which further confirms that Z factor varies along the riser. Unlike in the case of the variation of the profiles of the Z factors in Figure 8 where the profile for the correlation of Heidaryan et al., (2001a) is very close to the profile of the ideal gas, in Figure 9, the profile of viscosity for Bahadori (2007) is the closest to the profile of viscosity for the ideal gas.

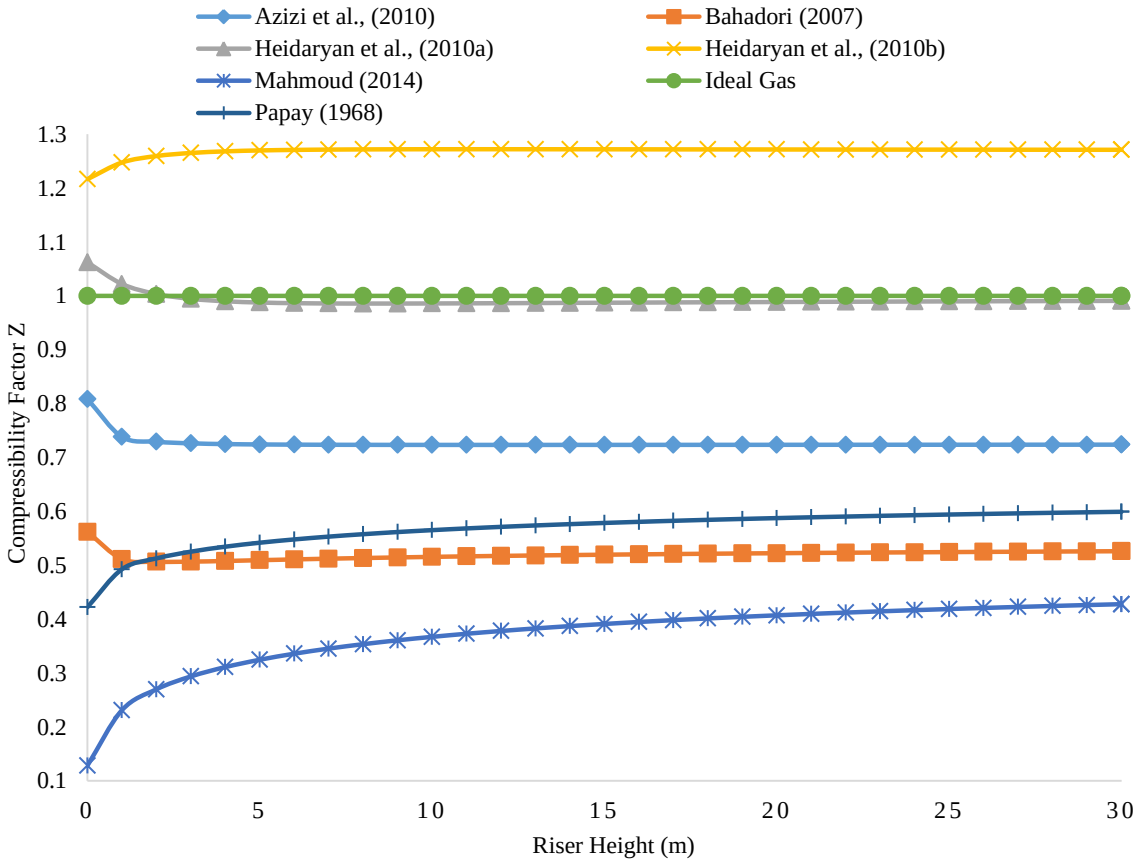

Figure 8: Various compressibility factor profiles

Figure 10 shows the profiles of the gas and catalyst phase temperatures as a function of the riser height for each Z factor correlation. The profiles for all the correlations in both the temperature of gas phase and catalyst phase vary from each other in the first 1 m to 5 m height of the riser showing the tendency of each Z factor correlation to be influenced by the temperature change in the riser, which means that different heats of reaction may prevail for different Z factors. This also shows that the heat balance in both the riser and regeneration is altered. However, looking at after a height of 5 m, the profiles tends to come together with almost similar outlet temperatures for both catalyst and gas phases, suggesting that the influence of the Z factor may be felt much only at the first few meters in the riser. The output

temperatures are within the limit of acceptability with temperatures of the profile for ideal gas Z factor. Again, it shows that Z factor affects the temperature profile.

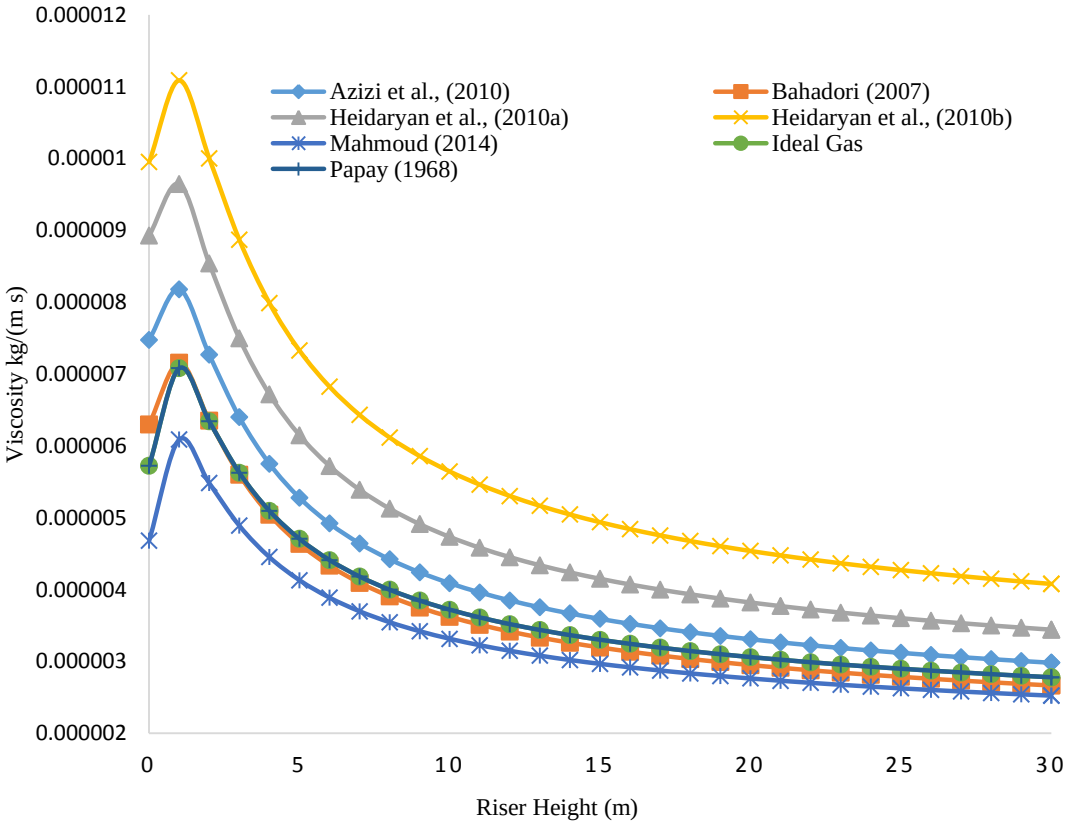

Figure 9: Viscosity profile along riser height

The temperature variation with Z factor also affects the yield of products from the cracking reactions. This is because the kinetic reactions are temperature dependent. Therefore, heat of reaction for the different Z factor correlation would eventually change accordingly. Figure 11 shows how gasoline and the converted gas oil varyalong the riser height for different Z factor correlations. Just as in the case of the temperature, where most of the interactions as a result of the different Z factors in the riser was centred at the first 5 m of the riser (Figure 10), the profiles of both gas oil and gasoline in Figure 11 show similar trends. The first few meters of the riser respond differently for different Z factor correlation, confirming that the right Z factor needs to be used in the simulation of the FCC unit. Although the yield of gasoline for all the Z factor correlations show some degree of consistency with the yield of gasoline for the ideal gas Z factor and the plant data, there are still small differences as shown in Table 4. The percentage differences between the gas oil and gasoline with ideal gas Z factor correlation and gas oil and gasoline with other Z factor correlations are an average of 1.21%

and 0.51% respectively. If these percentages were achieved on an existing conversion of gas oil and yield of gasoline under optimum operating conditions in the riser, it would amount to more yield of desired product and eventually increase profitability. These differences shown in Table 4 shows that every Z factor used in the riser yields different products.

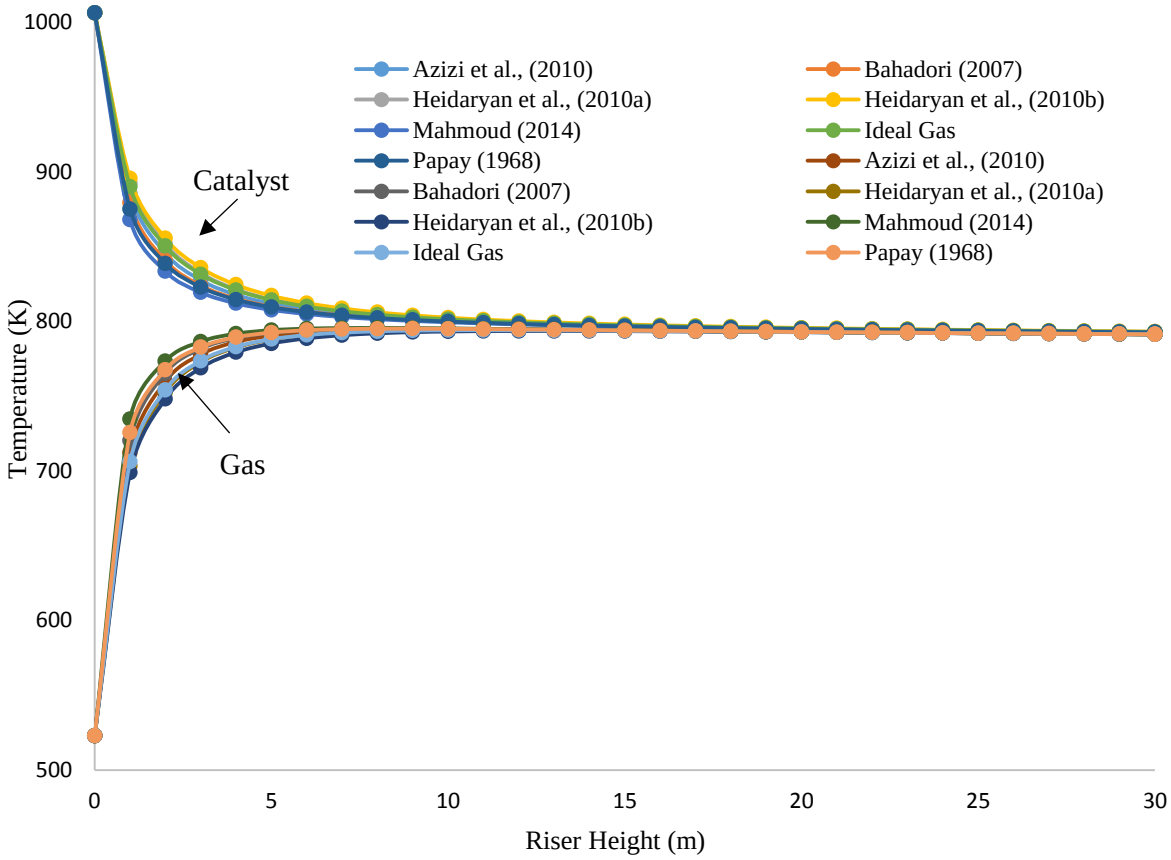

Figure 10: Temperature profiles of gas and catalyst phases

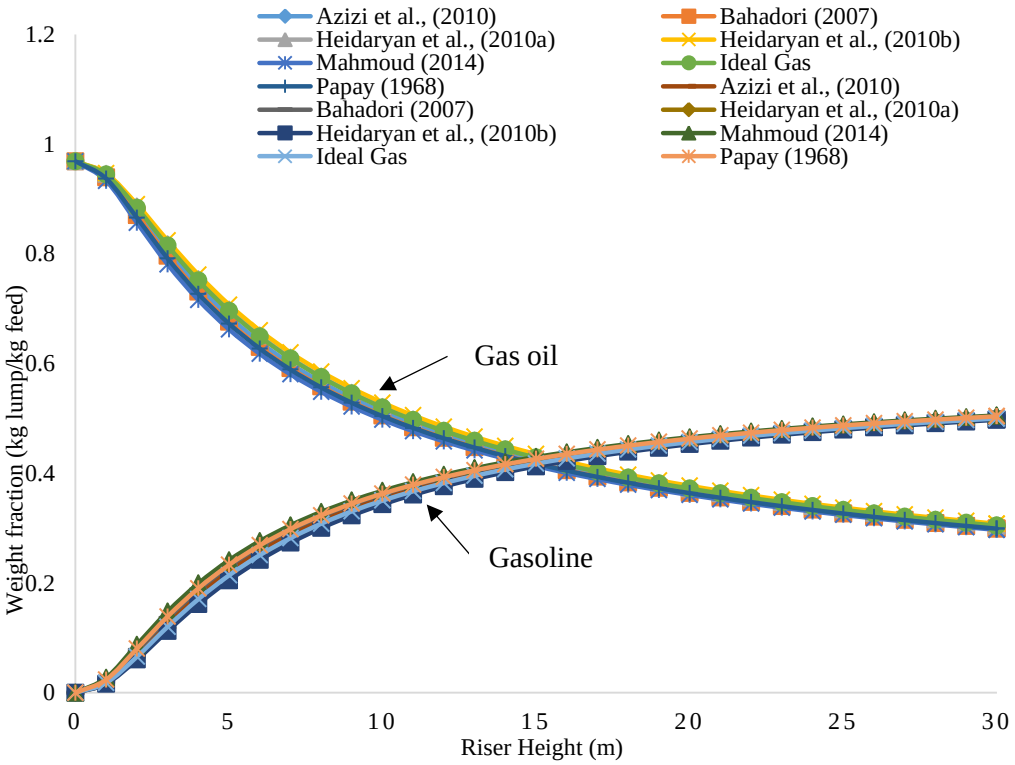

Figure 11: Profiles of gas oil and gasoline along the riser

Table 4: Gas oil and Gasoline fractions at the exit of the riser

Lump (kg lump/kg feed)	Gas oil	% Difference	Gasoline	% Difference
Azizi et al., (2010)	0.3014	1.02	0.5019	0.42
Bahadori (2007)	0.2991	1.82	0.5036	0.75
Heidaryan et al., (2010a)	0.3046	0.04	0.4996	-0.03
Heidaryan et al., (2010b)	0.3079	1.12	0.4974	-0.48
Mahmoud (2014)	0.2968	-2.60	0.5053	1.10
Ideal gas	0.3045	0.00	0.4998	0.00
Papay (1968)	0.2990	-1.85	0.5037	0.78
Han and Chung (2001b)	0.2735	-11.33	0.5085	1.71

In order to determine which Z factor correlation is suitable for the riser simulation, an important variable that controls the hydrodynamics of the riser, the riser pressure, was observed. The pressure variation was investigated for all the correlations and compared with the pressures from the models with ideal gas correlations, Kaduna refinery plant and Han and Chung (2001b). The pressures along the riser height for different Z correlations are shown in Figure 12, while the inlet and outlet pressures along with the pressure drops across the riser

length for each correlation are shown in Table 5. The pressure profiles in the riser for all the correlations including that with ideal gas, follow a similar pattern. They differ only in the inlet and outlet values. Plant data shows that the riser inlet pressure ranges from 230-270 kPa (Chiyoda 1980), while the simulation of Han and Chung (2001b) shows that the inlet pressure is about 246 kPa. Going by these inlet conditions, Figure 12 shows only the correlations with ideal gas Z = 1 and Heidaryan et al., (2010a) fall within the range given by Chiyoda (1980) and come close to 246 kPa. Hence, the model of Heidaryan et al., (2010a) can be considered suitable for the Z factor correlation in the riser simulation. The ideal gas correlation, which considered Z equal to one, even though it predicted the riser inlet pressure to be within the range given by Chiyoda (1980) and the 246 kPa, may not be suitable. This is because, according to the Han and Chung (2001b) simulation, the ideal gas pressure correlation does not vary along the riser length against the fact that the pseudo-reduced temperature and pseudo-reduced pressure (variables that depend on Z factor) do vary along the length of the riser (Pareek et al. 2003).

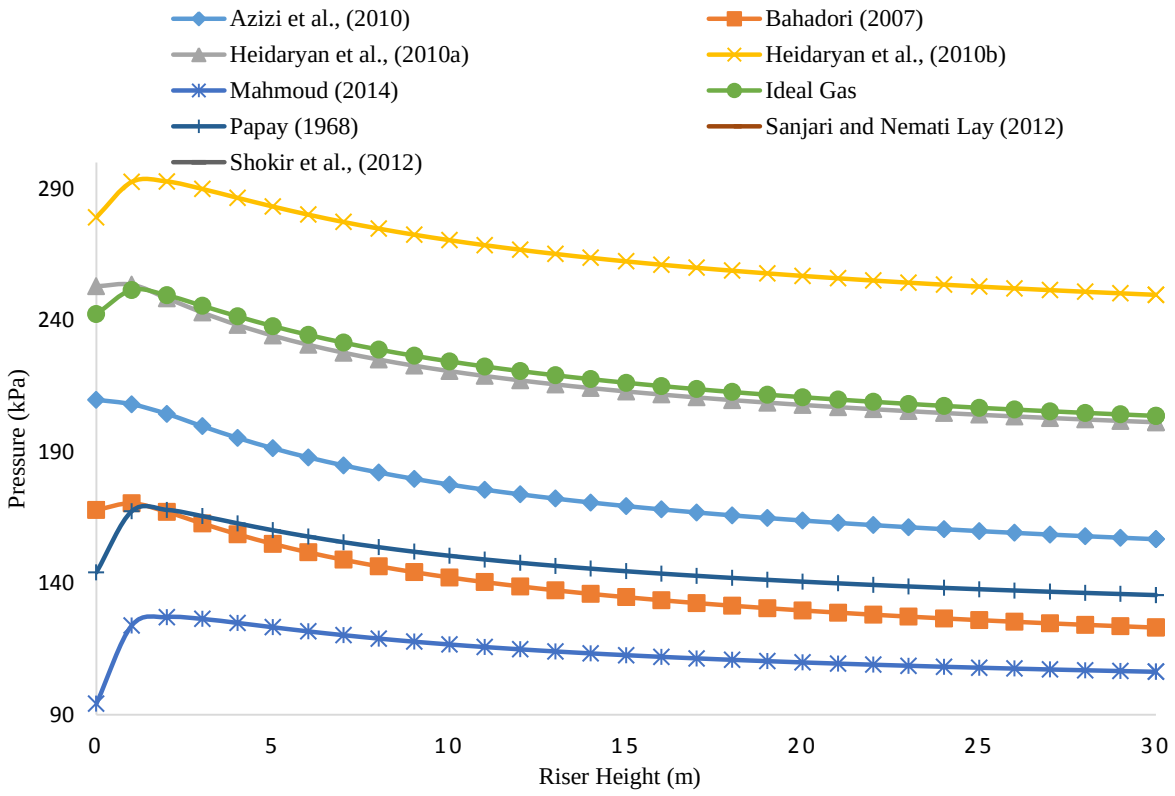

Figure 12: Pressure profiles for different Z factor correlations

Another aspect of the pressure profiles in Figure 12 to consider is the pressure drop. According to the Han and Chung (2001b) simulation, the pressure drop is 16 kPa as seen in Table 5.

Table 5: Riser pressure drop (DeltaP) for different Z factor correlations.

Pressure (kPa)	Riser inlet	Riser outlet	DeltaP	DeltaP (Han and Chung (2001b))	DeltaP Kaduna refinery
Azizi et al., (2010)	209.75	156.70	53.05	16.000	27.46
Bahadori (2007)	167.83	123.08	44.75	16.000	27.46
Heidaryan et al., (2010a)	252.88	201.18	51.70	16.000	27.46
Heidaryan et al., (2010b)	279.15	249.65	29.50	16.000	27.46
Mahmoud (2014)	94.12	106.27	-12.15	16.000	27.46
Ideal gas	242.32	203.60	38.72	16.000	27.46
Papay (1968)	144.10	135.45	8.65	16.000	27.46

The pressure drop in the industrial riser as seen in Table 5 is 27.46 kPa (Chiyoda 1980). Clearly, none of the pressure drops from the correlations in Table 5 came close to 16 kPa except that the pressure of 29.50 kPa from Heidaryan et al., (2010b) correlation is close to 27.46 kPa of Kaduna refinery (Chiyoda 1980). Even though the correlation of Heidaryan et al., (2010b) gave a closer pressure drop than the correlation of Heidaryan et al., (2010a), the latter correlation predicts the riser inlet pressure better and follows very closely the pressure profile of Z factor correlations with ideal gas and its Z factor profile as shown in Figure 13.

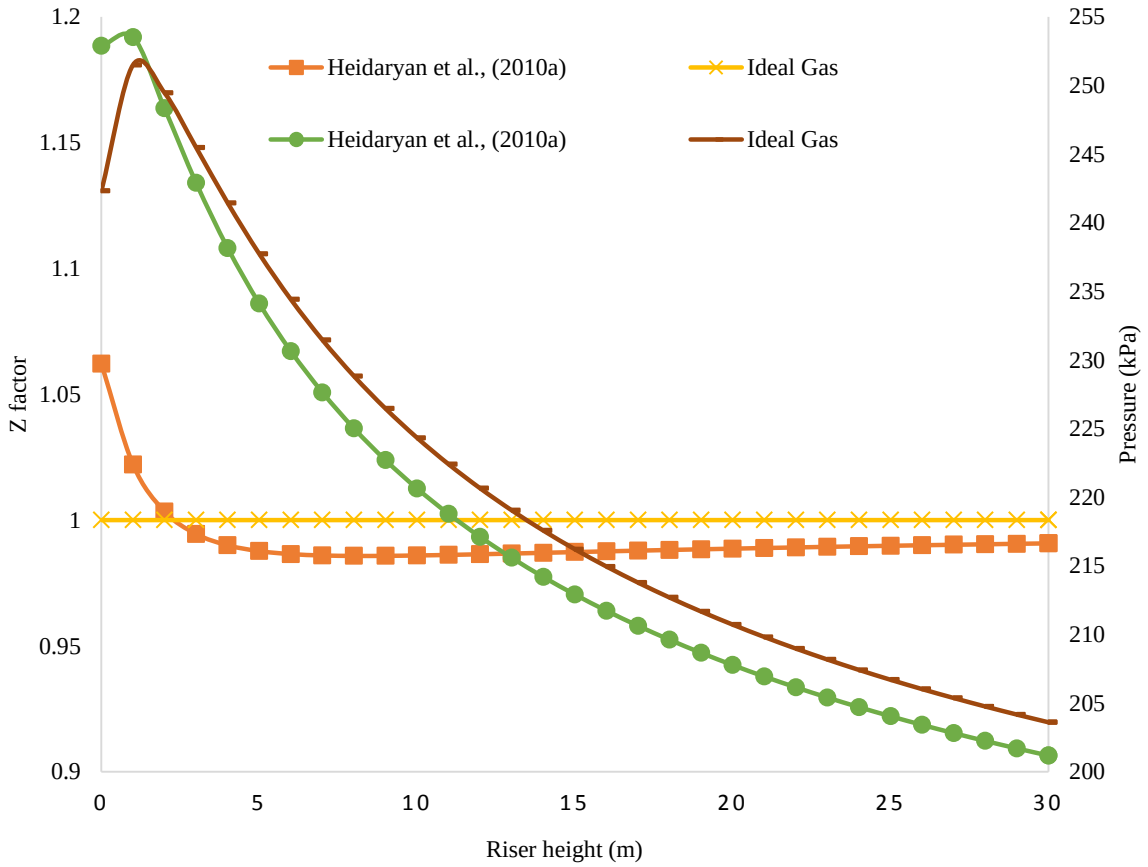

Figure 13: Pressure and velocity profiles along the riser

The difference between the pressures predicted by the riser model with Z factor correlation of Heidaryan et al., (2010a) and that of the ideal gas at the inlet of the riser is 10.25 kPa and at the outlet, it is -2.42 kPa. The difference between the Z factor predicted by the riser model with Z factor correlation of Heidaryan et al., (2010a) and that of the ideal gas at the inlet of the riser is 0.062 and at the outlet, it is -0.01. These differences are the least between any of the correlations. It is also the least difference between all the correlations and the two correlations of Heidaryan et al., (2010a) and that of the ideal gas at the inlet of the riser. Heidaryan et al., (2010a) and the ideal gas Z factor correlations predict the inlet pressure much closely to the plant inlet pressure (Chiyoda 1980), and the pressure of Han and Chung (2001b) model. Heidaryan et al., (2010a) Z factor correlation will be used for the riser simulation since it predicts the Z factor across the length of the riser.

To observe the behaviour of the Heidaryan et al., (2010a) Z factor correlation on varying catalyst-to-oil ratio (C/O) and varying riser diameter, four different C/O were used with a riser model that incorporates the Heidaryan et al., (2010a) Z factor correlation. Each C/O ratio was varied against the correlations of Heidaryan et al., (2010a) Z factor and that for the

ideal gas to see the impact on the pressures at inlet and the outlet. In addition, since most of the assumptions made in modelling the riser unit by considering its gas phase as ideal gas came from experiments with very small riser diameters, the Z factor impact is studied over varied industrial riser diameter.

Figure 14 shows the variation of pressure for Heidaryan et al., (2010a) Z factor correlations at different C/O ratios. All the profiles started at the riser inlet pressure of 252.88 kPa but behaved differently in the first 5 – 10 m of the riser and eventually level out. The varied behaviour at the beginning of the riser is because of the expansion of the gas phase caused by the high temperature and mixing from the vaporisation section. At C/O ratio of 8.085, the pressure decreases immediately after entering the riser. This is because, at higher mass flow rate of catalyst, the residence time is less and the expansion of the gas phase is distributed along the riser. When the C/O ratio is decreased to 4.085, mass flowrate of catalyst is decreased, causing brief accumulation of catalyst at the bottom of the riser (Das et al. 2007). Hence, the residence time for catalyst at the bottom of the riser slightly increased to allow more heat to be absorbed from the catalyst for the vaporization, causing the gas oil in contact with the catalyst to expand much more. This is the reason for the rise in the pressure profile.

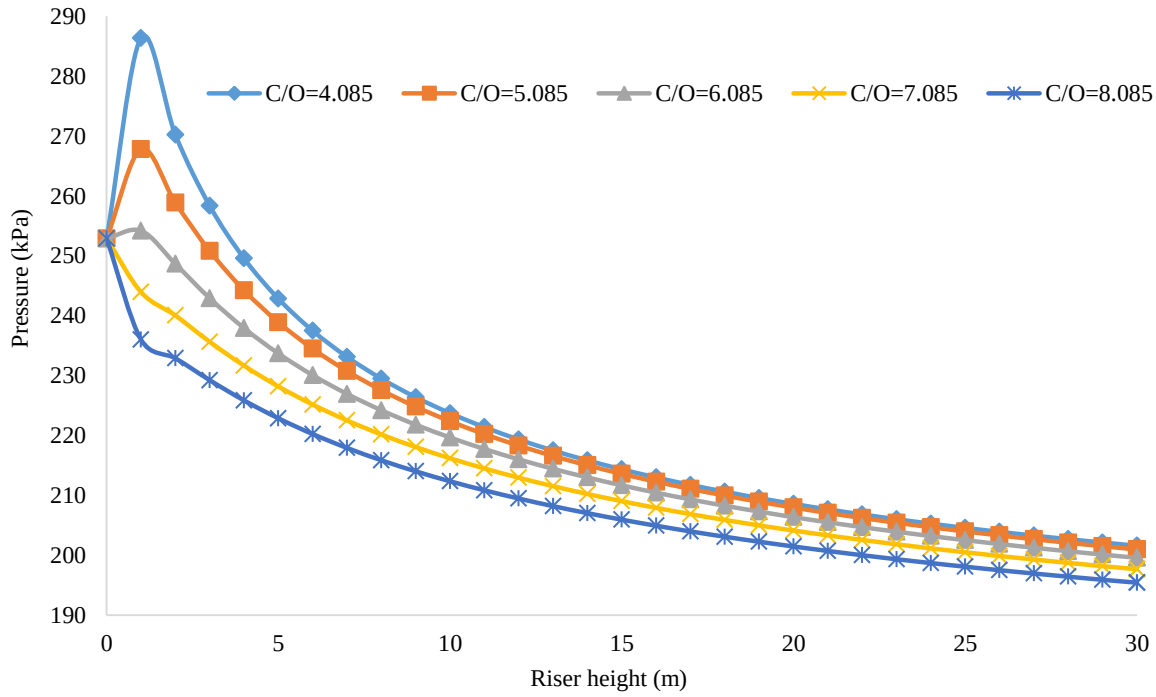

Figure 14: Pressure profiles for different C/O with Z factor correlation

This trend is also followed in Figure 15 for the variation of pressure for the ideal gas Z factor correlations, and at different C/O ratios. The first 5 m of the riser shows a higher interaction

of the pressure for lower C/O ratio 4.085 where the inlet pressure is 242.32 kPa but shoots up to 283.6 kPa in the first 1 m before it decreases and levels out. This is due to brief accumulation of catalyst at the bottom of the riser at this C/O ratio (Das et al. 2007). Unlike the low interaction observed for the higher C/O ratio 8.085 where the inlet pressure 242.32 kPa drops to 233.05 kPa before it eventually levels out. The pressure profiles for the Heidaryan et al., (2010a) Z factor correlation in Figure 14 levels out evenly without the overlap observed in Figure 15 for the pressure profiles of the ideals gas Z factor. Therefore, the pressure drops for the two Z factor correlations at different C/O ratio were obtained and presented in Table 6.

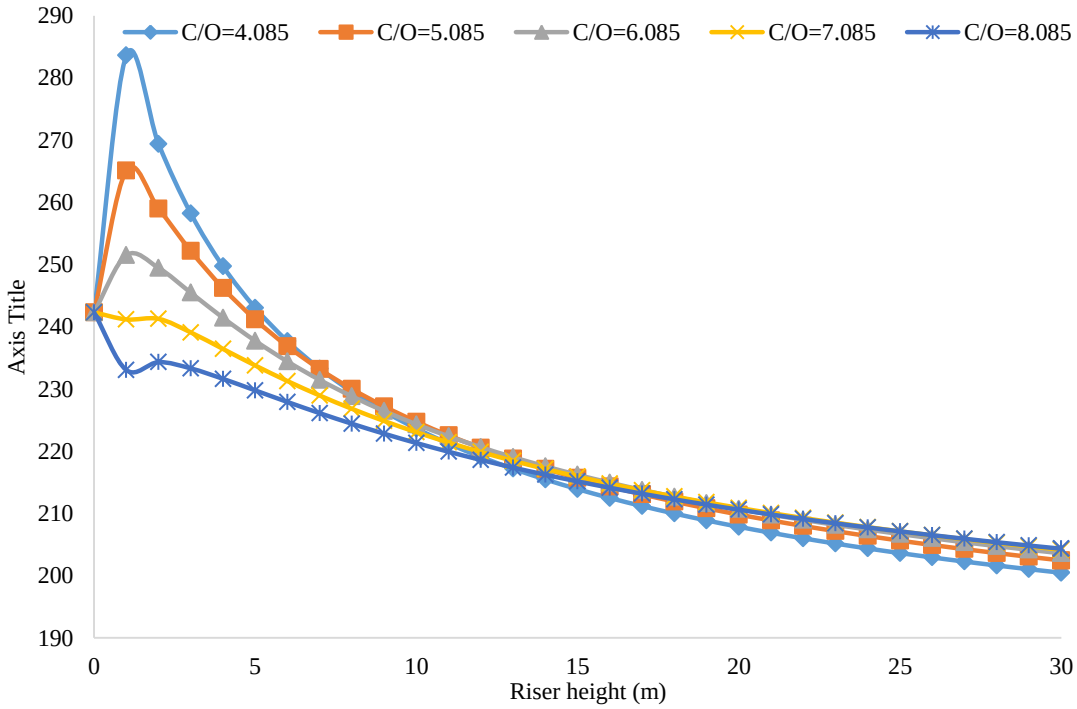

Figure 15: Pressure profiles along riser height for different C/O for Z = 1

Table 6 shows pressure measurements for two correlations, Heidaryan et al., (2001a) Z factor correlation and the ideal gas Z factor, Z = 1, at different C/O ratios. Values at C/O ratios of 9.085 and 10.085 were obtained to find out if the pressure drop for the ideal gas Z factor correlation, continue to drop after C/O ratio 8.085. The variation of the pressure drop with C/O ratios are presented in Figure 16.

Table 6: Pressures for different Z factor correlations at different C/O ratio.

C/O ratio	Pressure with Heidaryan et al., (2001a)			Pressure with Z factor = 1		
	Riser inlet	Riser outlet	DeltaP	Riser inlet	Riser outlet	DeltaP
4.085	252.88	201.58	51.30	242.32	200.47	41.85
5.085	252.88	200.96	51.92	242.32	202.45	39.87
6.085	252.88	199.57	53.31	242.32	203.60	38.72
7.085	252.88	197.67	55.21	242.32	204.17	38.15
8.085	252.88	195.41	57.47	242.32	204.33	37.99
9.085	252.88	192.91	59.97	242.32	204.20	38.12
10.085	252.88	190.23	62.65	242.32	203.86	38.46

The pressure drop at different C/O for the two correlations were investigated to observe the behaviour of the Z factor as it affect the pressure drop at every C/O. It can be seen from Figure 16 that the pressure drop for the ideal gas Z factor correlation decreased nonlinearly from 41.85 kPa across the riser height at C/O ratio of 4.085 to a minimum of 37.99 kPa at 8.085 before rise up again. This is not the case with the pressure drop observed with the Z factor correlation of Heidaryan et al., (2001a), where the pressure drop continues to rise polynomially from a value of 51.30 kPa across the riser height at C/O ratio of 4.085 without any minimum. A pressure drop of 163 kPa across the riser height has been reported in the literature (Chang et al. 2012; Pelissari et al. 2016) and a variation between 200 kPa and 250 kPa across the riser height over a period of 69 hours was also reported (Pinho et al. 2017).

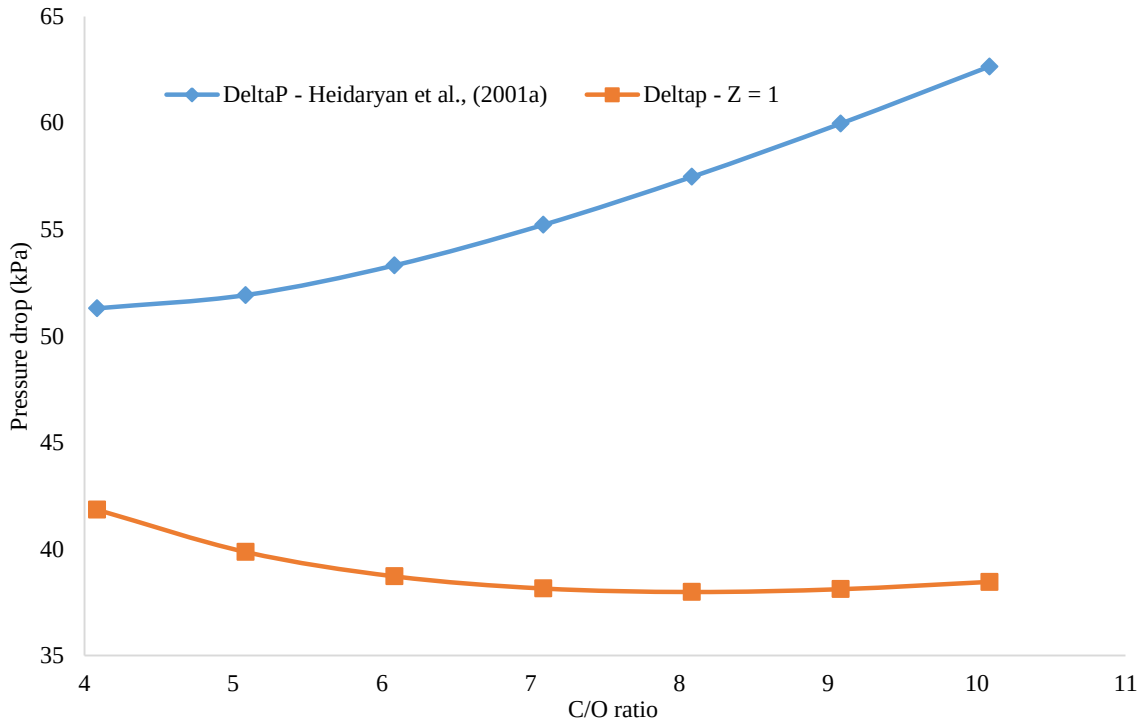

Figure 16: Pressure drop at different C/O ratio

Using the statistical modelling approach, trendlines obtained from the curves in Figure 16 show that the pressure drop can be predicted as a function of the C/O ratio from the following polynomial equations of fourth order with both equations having a coefficient of determination, $R^2 = 1$.

For the Z factor correlation of Heidaryan et al., (2001a), the equation is

$$\Delta P = 0.0026\,(C/O)^4 - 0.0969\,(C/O)^3 + 1.4539\,(C/O)^2 - 7.5762\,(C/O) + 63.872 \quad (66)$$

For the Z factor correlation of ideal gas Z = 1, the pressure drop equation is

$$\Delta P = 0.0025\,(C/O)^4 - 0.0958\,(C/O)^3 + 1.4864\,(C/O)^2 - 10.514\,(C/O) + 65.827 \quad (67)$$

Once a C/O ratio is known, these equations can provide the pressure drop values across the riser height in meters.

Figure 17 shows the variation of Z factor of Heidaryan et al., (2001a) along the riser for different C/O ratios. The Z factor for an ideal gas would remain constant at 1.0 across the length of the riser. Figure 17 shows that the Z factor is not constant across the length of the riser because pseudo-reduced pressure and pseudo-reduced temperature vary from the

bottom to the top (Pareek et al. 2003). This understanding may be of particular interest for the engineers when designing the riser.

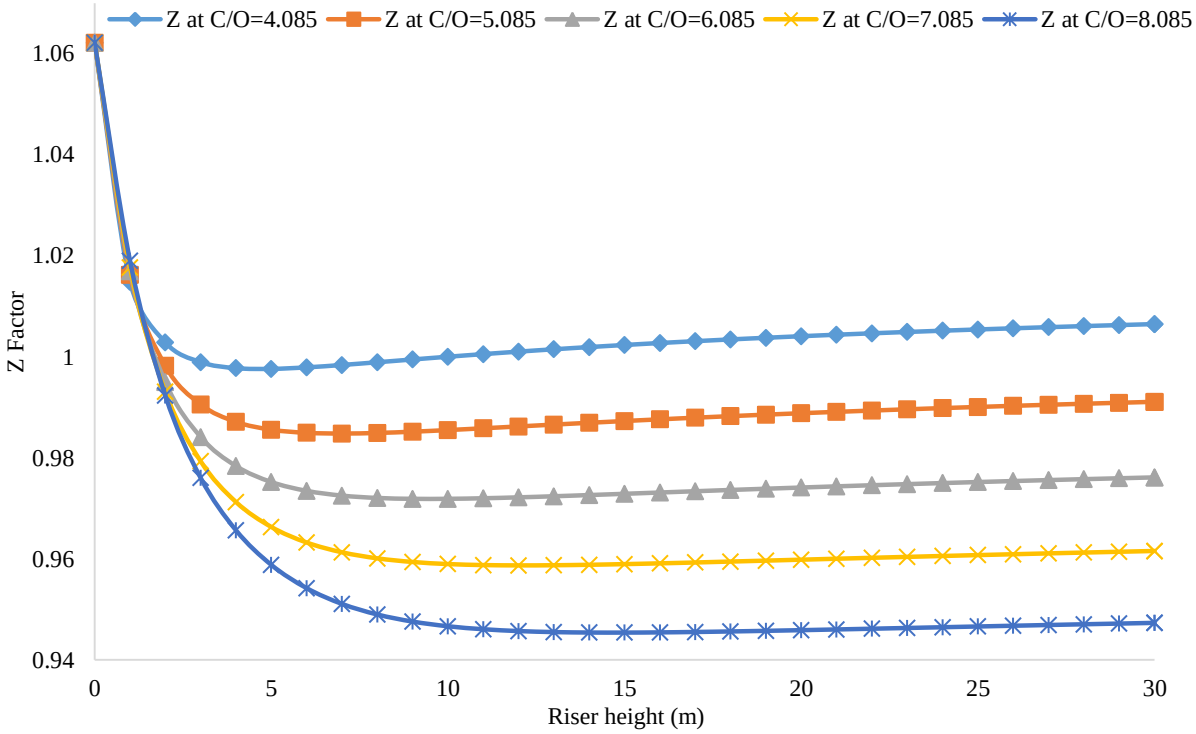

Figure 17: Z Factor correlation of Heidaryan et al., (2001a) at different C/O

In Figure 17, the Z factor at riser inlet for all C/O ratios is 1.0621, which would be different in the case of the ideal gas being constant Z = 1 at inlet and at any point in the riser. At C/O ratio of 8.085, the Z factor at the exit of the riser is 0.9473 while at C/O ratio 4.085 the Z factor at the exit of the riser is 1.0065. This shows that the higher the C/O ratio, the further the Z factor profile and exit value from other C/O ratios Z factor profiles and exit values. It is also further away from what was considered for the ideal gas Z = 1 constant across the riser length. To obtain a statistical model for this relationship, Z factors at the exit of the riser for C/O ratios 9.085 and 10.085 at the same process conditions were obtained and presented along with other C/O ratios in Table 7.

Table 7: Z factor correlation of Heidaryan et al., (2001a) at different C/O ratio.

C/O ratio	Z factor of Heidaryan et al., (2001a)		
	Riser inlet	Riser outlet	Delta Z
4.085	1.06	1.01	0.05
5.085	1.06	0.99	0.07
6.085	1.06	0.98	0.08
7.085	1.06	0.96	0.10
8.085	1.06	0.95	0.11
9.085	1.06	0.93	0.13
10.085	1.06	0.92	0.14

The Z factor change for each C/O ratio at the riser inlet and outlet is also present in Table 7. It shows that the higher the C/O ratio, the higher the Z factor. This also confirms that Z factor vary with C/O ratios and not constant for all C/O ratios as always considered in the literature. Figure 18 shows how change in Z factor varies with the C/O ratios. A statistical correlation with $R^2 = 1$ is obtained for the varying Z factor with C/O ratio and given as:

$$Delta\ Z = -0.0002\ (C/O)^2 + 0.0169\ (C/O) - 0.0104 \quad (68)$$

Once the inlet Z factor is known, the change in Z can be obtained at a given C/O ratio, which will eventually lead to the exit Z factor from the difference. It also shows the extent in numerical terms how the real Z factor varies from the ideal gas phase Z factor.

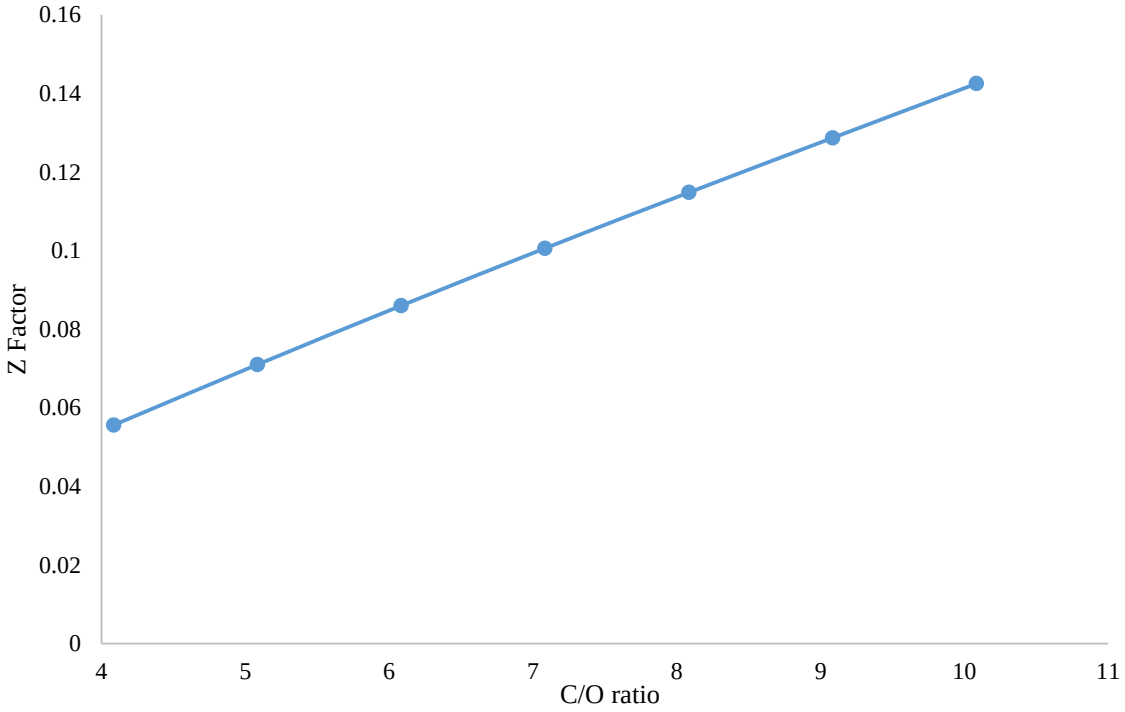

Figure 18: Z factor at various C/O

Figure 19 presents the pressure profile for different riser diameters for Z factor correlation of Heidaryan et al., (2001a) and Z factor correlation of ideal gas at a C/O ratio of 6.085. This is to find out the pressure drop at larger diameter because experiments that informed the assumptions to treat the gas phase as an ideal gas came from very small diameter risers.

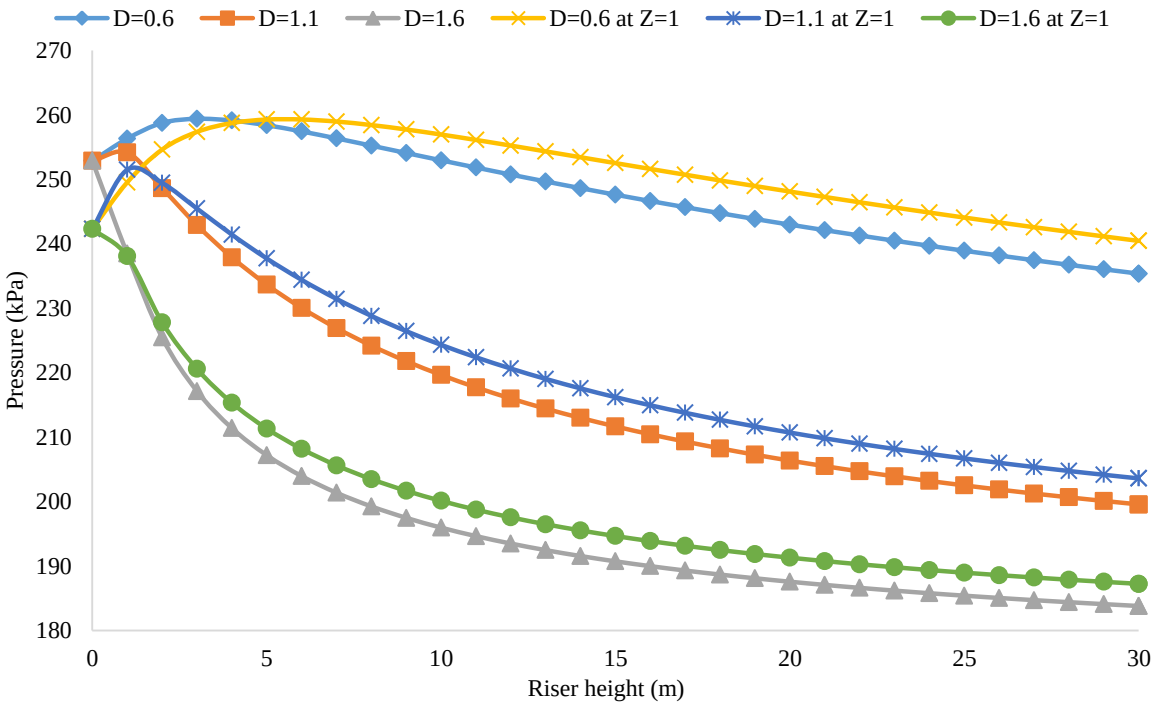

Figure 19: Pressure profile for different diameters at different Z factor correlation

At lower riser diameter of 0.6 m, the pressure profiles for both Z factor of ideal gas and Heidaryan et al., (2001a) show lower pressure drops as shown in Table 8. When the diameter was increased to 1.1 m and 1.6 m, the pressure drop increased for both profiles and Z factors also shown in Table 8.

Table 8: Z factor correlation of Heidaryan et al., (2001a) at different C/O ratio.

Riser diameter (m)	Z factor	Pressures (kPa)		
		Riser inlet	Riser outlet	Delta P
0.60	Heidaryan et al., (2001a)	252.88	235.38	17.50
	Ideal gas Z = 1	242.32	240.46	1.86
1.1	Heidaryan et al., (2001a)	252.88	199.57	53.31
	Ideal gas Z = 1	242.32	203.60	38.72
1.6	Heidaryan et al., (2001a)	252.88	183.78	69.10
	Ideal gas Z = 1	242.32	187.24	55.08

The pressure drop increases as the diameter increases as stated in the literature (Santos et al. 2007) and as seen in Figure 20. The profile of the pressure drop that represents the Z factor of Heidaryan et al., (2001a) has higher pressure drops than the profile for the Z factor of the

ideal gas. Though both profiles follow a similar pattern, it is clear that the Z factor of Heidaryan et al., (2001a) correlation affects the pressure regime in the riser.

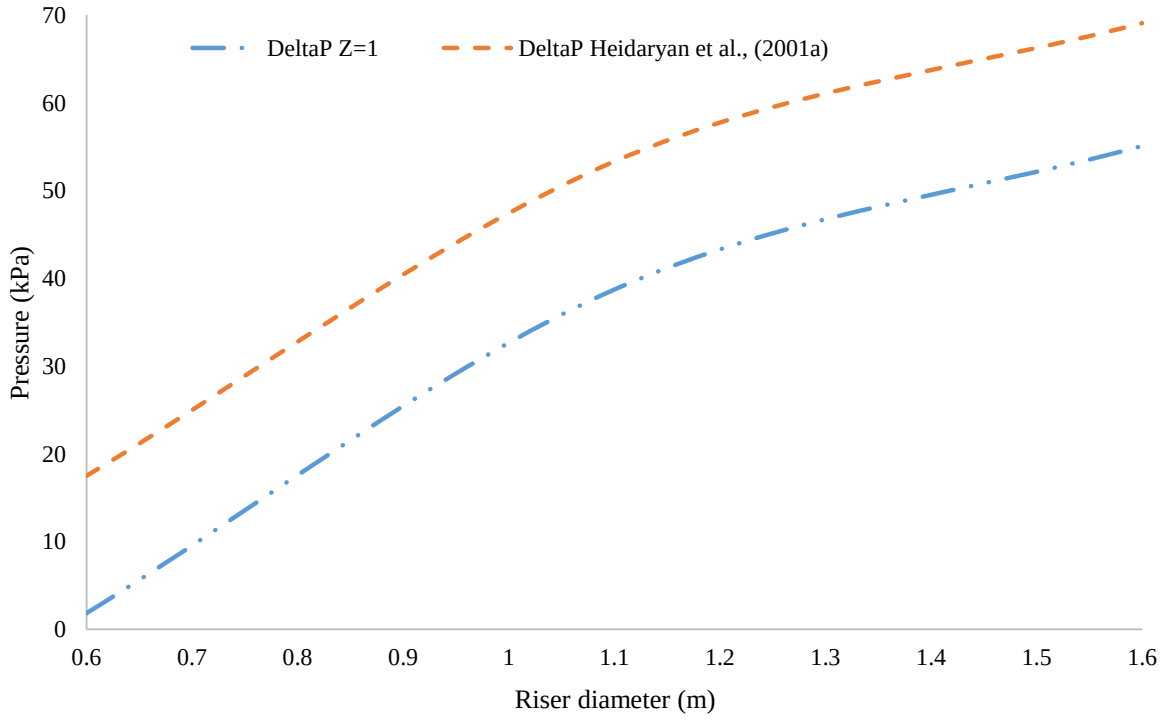

Figure 20: Pressure drop across the riser at different diameters for different Z factors

Figure 21 shows the Z factor correlations of Heidaryan et al., (2001a) profile for different riser diameters at a C/O ratio of 6.085. For the three risers with different diameters, the Z factor at the entrance of the riser is 1.06 and decreases to an average of Z factor 0.97. The profile for the 0.6 m diameter riser descended smoothly to a Z factor of 0.97 in the first 13 m of the riser. The Z factor profiles for 1.1 m and 1.6 m diameter riser descended sharply and reached the average Z factor of 0.97 in the first 5 m. Clearly, from Figure 21, the Z factor correlation of Heidaryan et al., (2001a) behave differently as the diameter of the riser increases. Therefore, every riser may have its different Z factor profile because of its diameter.

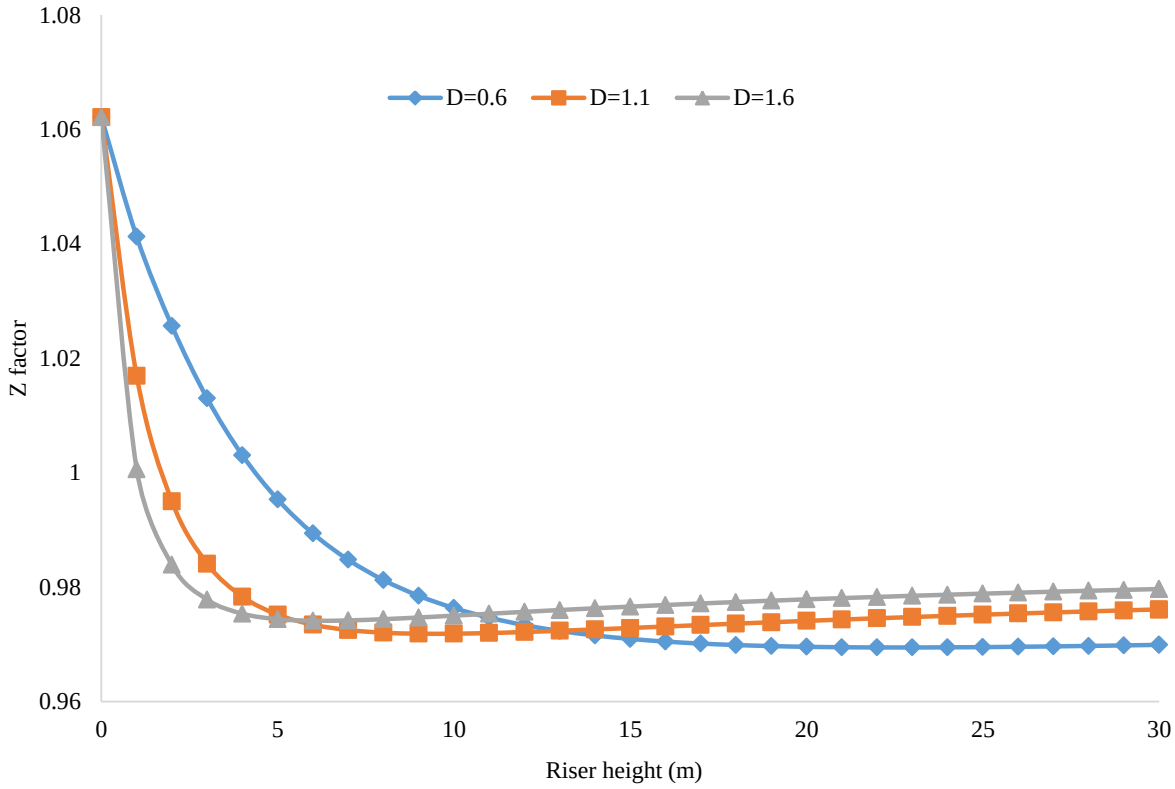

Figure 21: Profile of Z factor of heidaryan et al., (2001a) along the riser

5. Conclusions

In this work, a steady state detailed FCC riser process model is for the first time simulated with different Z factor correlations implemented on gPROMS software. A 4-lump kinetic model is used where gas oil cracks to form gasoline, coke and gases. The following conclusions can be made:

- The simulation results from this work compare favourably with the results obtained by Han and Chung (2001a, b) where the model of the riser was adopted, and with plant data. Thus demonstrating the capability of the gPROMS software in simulating the riser of the FCC unit. Hence, gPROMS can be recommended for the simulation of the entire FCC unit.
- The Heidaryan et al., (2010a) Z factor correlation is suitable in representing the Z factor across the riser.
- Using different Z factors in the simulation of the riser with the same process conditions yields different profiles for some process variables such viscosity of gas phase, heat of reaction due to varying temperature profiles and varying compositions at every point in the riser.
- The pressure at every point in the riser is different for different C/O ratios. The pressure is also different at every point when the Heidaryan et al., (2010a) Z factor correlation is used as opposed to when the gas phase is treated as an ideal gas.

- When operating an industrial riser, increase in pressure drop follows a polynomial function at varying C/O ratios.
- The higher the C/O ratio, the further away the gas phase behaves from the ideal gas.
- The higher the C/O ratio, the higher the change in Z factor between the inlet and outlet Z factor of the riser.
- A correlation is developed to measure the magnitude of deviation of the gas phase from ideal gas.
- Every riser has a different pressure profile and Z factor profile depending on the riser diameter.

Notation

A	Surface area, m^2
A_{ptc}	Effective interface heat transfer area per unit volume, m^2/m^3
C	Mole concentration, kg mole/m^3
C_{p_g}	Gas heat capacity, kJ/kg K
C_{p_s}	Solid heat capacity, kJ/kg K
D	Diameter, m
d_c	Catalyst average diameter, m
E	Activation energy, kJ/kg mole
F	Mass flow rate, kg/s
H	Specific enthalpy, kJ/kg
ΔH	Heat of reaction kJ/kg
ΔH_{vlg}	heat of vaporization of liquid feedstock in the feed vaporization section, kJ/kg
h	Enthalpy of reaction kJ/kg
h_p	Interface heat transfer coefficient between the catalyst and gas phases
h_T	Interface heat transfer coefficient, kJ/m^2 s K
k_{i0}	Frequency factor in the Arrhenius expression, 1/s
K_i	Rate coefficient of the four-lump cracking reaction, 1/s
K_g	Thermal conductivity of hydrocarbons
L	Length, m
M_w	Molecular weight
P	Pressure, kPa
Q_{react}	Rate of heat generation or heat removal by reaction, kJ/s

R	Ideal gas constant, 8.3143 kPa m^3/-kg mole K or kJ/kg mole K
RAN	Aromatics-to-naphthenes ratio in liquid feedstock
S_c	Average sphericity of catalyst particles
S_g	Total mass interchange rate between the emulsion and bubble phases, 1/s
T	Temperature, K
u	superficial velocity, m/s
V	Volume, m^3
y	Weight fraction
Z	Gas compressibility factor or Z factor

Greek

Ω	Cross-sectional area
ρ	Density, kg/m^3
∅	Catalyst deactivation function
ε	Voidage
α	Catalyst deactivation coefficient
α_C^*	exponent for representing α
μ_g	viscosity

Subcript

Cc	Coke on catalyst
CL1	Cyclone 1
ck	Coke
ds	Disperse steam
FS	Feed vaporization section
g	Acceleration m/s^2
gl	gasoline
go	Gas oil
gs	gases
MABP	Molal average boiling temperature, K
MeABP	Mean average boiling temperature, K
pc	pseudo-critical
pr	pseudo-reduced

Rs	Riser
RT	Disengager-stripping section

Appendix A

Table A.1 and Equations A1 – A24 are correlations of physical and transport parameters adopted from the literature (Han and Chung 2001a; Han and Chung 2001b).

Table A.1: Distillation Coefficients

Volume % distilled	10	30	50	70	90
a	0.5277	0.7429	0.8920	0.8705	0.9490
b	1.0900	1.0425	1.0176	1.0226	1.0110

Table A.2: Tuned coefficients for Z factor (Azizi et al. 2010)

Coefficient	Tuned Coefficient	Coefficient	Tuned Coefficient
a	0.0373142485385592	k	−24449114791.1531
b	−0.0140807151485369	l	19357955749.3274
c	0.0163263245387186	m	−126354717916.607
d	−0.0307776478819813	n	623705678.385784
e	13843575480.943800	o	17997651104.3330
f	−16799138540.763700	p	151211393445.064
g	1624178942.6497600	q	139474437997.172
h	13702270281.086900	r	−24233012984.0950
i	−41645509.896474600	s	18938047327.5205
j	237249967625.01300	t	−141401620722.689

Table A.3: Tuned coefficients for Z factor (Bahadori et al. 2007)

Coefficient	Tuned coefficients
Aa	0.969469
Ba	−1.349238
Ca	1.443959
Da	−0.36860
Ab	−0.107783
Bb	−0.127013
Cb	0.100828
Db	−0.012319
Ac	0.018481
Bc	0.052341
Cc	−0.050688
Dc	0.01087
Ad	−0.000584
Bd	−0.002146
Cd	0.002096
Dd	−0.000459

Table A.4: Tuned coefficients for $0.2 \leq P_{pr} \leq 3$ (Heidaryan et al. 2010a)

Coefficient	Tuned Coefficient
A1	2.827793
A2	-0.4688191
A3	−1.262288
A4	−1.536524
A5	−4.535045
A6	0.06895104
A7	0.1903869
A8	0.6200089
A9	1.838479
A10	0.4052367
A11	1.073574

Table A.5 Tuned coefficients for Z factor (Heidaryan et al. 2010b)

Coefficient	Tuned Coefficient
A1	1.11532372699824
A2	−0.07903952088760
A3	0.01588138045027
A4	0.00886134496010
A5	−2.16190792611599
A6	1.15753118672070
A7	−0.05367780720737
A8	0.01465569989618
A9	−1.80997374923296
A10	0.95486038773032

Table A.6: Tuned coefficients for Z factor (Sanjari and Lay 2012)

Coefficient	Tuned Coefficient
A1	0.007698
A2	0.003839
A3	−0.467212
A4	1.018801
A5	3.805723
A6	−0.087361
A7	7.138305
A8	0.083440

Heat capacity of gas, C_{pg}, is

$$C_{pg} = \beta_1 + \beta_2 T_g + \beta_3 T_g^2 \quad \text{(A.1)}$$

Where β_1, β_2, β_3 and β_4 catalyst decay constant given as

$$\beta_1 = -1.492343 + 0.124432K_f + \beta_4\left(1.23519 - \frac{1.04025}{S_g}\right) \quad \text{(A.2)}$$

$$\beta_2 = (-7.53624 \times 10^{-4})\left[2.9247 - (1.5524 - 0.05543K_f)K_f + \beta_4\left(6.0283 - \frac{5.0694}{S_g}\right)\right] \quad \text{(A.3)}$$

$$\beta_3 = (1.356523 \times 10^{-6})(1.6946 + 0.0884\beta_4) \quad \text{(A.4)}$$

$$\beta_4 = \left[\left(\frac{12.8}{Kf} - 1\right)\left(1 - \frac{10}{Kf}\right)(S_g - 0.885)(S_g - 0.7)(10^4)\right]^2 \text{ For } 10 < Kf < 12.8 \quad \text{(A.5)}$$

Else $\beta_4 = 0$ for all other cases

Kf is the Watson characterization factor written as

$$Kf = \frac{(1.8T_{MeABP})^{\frac{1}{3}}}{S_g} \quad \text{(A.6)}$$

Where M_{wg} is the molecular weight of the gas and can be calculated using

$$M_{wg} = 42.965\left[\exp\left(2.097 \times 10^{-4}T_{MeABP} - 7.787S_g + 2.085 \times 10^{-3}T_{MeABP}S_g\right)\right](T_{MeABP}^{1.26007}\ S_g^{4.98308}) \quad \text{(A.7)}$$

$$T_{MeABP} = T_{VABP} - 0.5556\exp[-0.9440 - 0.0087(1.8T_{VABP} - 491.67)^{0.6667} + 2.9972(Sl)^{0.3333} \quad \text{(A.8)}$$

Where T_{VABP} , the volume average boiling temperature and (Sl) is slope given as

$$(Sl) = 0.0125(T_{90ASTM} - T_{10ASTM}) \quad \text{(A.9)}$$

$$T_{VABP} = 0.2(T_{10ASTM+}\ T_{30ASTM+}T_{50ASTM+}\ T_{70ASTM+}\ T_{90ASTM}) \quad \text{(A.10)}$$

The ASTM D86 distillation temperatures are calculated using

$$T_{10ASTM} = a_{10}^{-\frac{1}{b_{10}}}(T_{10TBP})^{\frac{1}{b_{10}}} \quad \text{(A.11)}$$

$$T_{30ASTM} = a_{30}^{-\frac{1}{b_{30}}}(T_{30TBP})^{\frac{1}{b_{30}}} \quad \text{(A.12)}$$

$$T_{50ASTM} = a_{50}^{-\frac{1}{b_{50}}}(T_{50TBP})^{\frac{1}{b_{50}}} \quad \text{(A.13)}$$

$$T_{70ASTM} = a_{70}^{-\frac{1}{b_{70}}}(T_{70TBP})^{\frac{1}{b_{70}}} \quad \text{(A.14)}$$

$$T_{90ASTM} = a_{90}^{-\frac{1}{b_{90}}}(T_{90TBP})^{\frac{1}{b_{90}}} \quad (A.15)$$

Where a_i and b_i are distillation coefficients (Table A.1) and T_{iTBP} is the TBP distillation temperature.

Interface heat transfer coefficient between the catalyst and gas phases, h_p,

$$h_p = 0.03\frac{K_g}{d_c^{\frac{2}{3}}}\left[\frac{|(v_g - v_c)|\rho_g\varepsilon_g}{\mu_g}\right]^{\frac{1}{3}} \quad (A.16)$$

Thermal conductivity of hydrocarbons

$$K_g = 1 \times 10^{-6}(1.9469 - 0.374M_{wm} + 1.4815 \times 10^{-3}M_{wm}^2 + 0.1028T_g) \quad (A.17)$$

M_{WM} is the mean molecular weight of the combined catalyst and gas

$$M_{WM} = \frac{1}{\left(\frac{ygo}{M_{wgo}} + \frac{ygl}{M_{wgl}} + \frac{ygs}{M_{wgs}} + \frac{yck}{M_{ck}}\right)} \quad (A.18)$$

$$M_{wgo} = M_{wg} \quad (A.19)$$

$$M_{wgs} = 0.002M_{wH_2} + 0.057M_{wC_1} + 0.078M_{wC_2} + 0.297M_{wC_3} + 0.566M_{wC_4} \quad (A.20)$$

The viscosity of the gas

$$\mu_g = 3.515 \times 10^{-8}\mu_{pr}\frac{\sqrt{M_{WM}P_{pc}^{\frac{2}{3}}}}{T_{pc}^{\frac{1}{6}}} \quad (A.21)$$

$$\mu_{pr} = 0.435\exp\left[\left(1.3316 - T_{pr}^{0.6921}\right)P_{pr}\right]T_{pr} + 0.0155 \quad (A.22)$$

$$T_{pc} = 17.1419\left[\exp\left(-9.3145 \times 10^{-4}T_{MeABP} - 0.5444S_g + 6.4791 \times 10^{-4}T_{MeABP}S_g\right)\right] \times T_{MeAB}^{-0.4844}S_g^{4.0846} \quad (A.23)$$

$$P_{pc} = 4.6352 \times 10^{6}\left[\exp\left(-8.505 \times 10^{-3}T_{MeABP} - 4.8014S_g + 5.749 \times 10^{-3}T_{MeABP}S_g\right)\right] \times T_{MeAB}^{-0.4844}S_g^{4.0846} \quad (A.24)$$

Table A.7 summarizes the variables, feed and catalyst characteristic and other parameters used in this simulation. Most of the parameters were obtained from the industry and literature (Han and Chung 2001b; Ahari et al. 2008; John et al. 2017b).

Table A.7: Specifications of constant parameters and differential variables at $x = 0$.

Variable	Value
Riser Height, x (m)	30
$T_g(0)$ (Temperature of gas oil, K)	535
$T_c(0)$ (Temperature of gas catalyst, K)	933
$v_c(0)$ Velocity of catalyst (m/s)	12
$v_g(0)$ Velocity of gas oil (m/s)	10
D Riser Diameter (m)	1.1
F_c (Catalyst mass flowrate, kg/s)	300
F_g (Gas oil mass flowrate, kg/s)	49.3
$y_{go}(0)$ Mass fraction of gas oil	1.0
$y_{gl}(0)$ Mass fraction of gas oil	0.0
$y_{gs}(0)$ Mass fraction of gas oil	0.0
$y_{ck}(0)$ Mass fraction of gas oil	0.0
M_{wgo} Molecular weight gas oil (kg/k mol)	371
M_{wgl} Molecular weight gasoline (kg/k mol)	106.7
M_{wck} Molecular weight coke (kg/k mol)	14.4
d_c (Average particle diameter, m)	0.00007
S_c (Average sphericity of catalyst particles)	0.72
S_g (Specific gravity)	0.897
C_{ckCL1} (Coke on catalyst, kg coke/kg catalyst)	0.001
α_{c0} (pre-exponential factor of α_c)	1.1e-5
α_{c*} (Catalyst deactivation coefficient)	0.1177
C_{pc} (Heat capacity of catalyst, kJ/kg K)	1.15
ρ_c (Density of catalyst, kg/m^3)	1410
R_{AN}(Aromatics/Naphthenes in liquid feedstock)	2.1
T_{10TBP} TBP distilled 10 volume%, ^oC	554.3
T_{30TBP}, TBP distilled 30 volume %, ^oC	605.4
T_{50TBP}, TBP distilled 50 volume %, ^oC	647.0

T_{70TBP} TBP distilled 70 volume %, ^{o}C	688.2
T_{90TBP} TBP distilled 90 volume %, ^{o}C	744.8
a_{10} Distillation Coefficients 10 volume%	0.5277
a_{30} Distillation Coefficients 30 volume %	0.7429
a_{50} Distillation Coefficients 50 volume %	0.8920
a_{70} Distillation Coefficients 70 volume %	0.8705
a_{90} Distillation Coefficients 90 volume %	0.9490
b_{10} Distillation Coefficients 10 volume %	1.0900
b_{30} Distillation Coefficients 30 volume %	1.0425
b_{50} Distillation Coefficients 50 volume %	1.0176
b_{70} Distillation Coefficients 70 volume %	1.0226
b_{90} Distillation Coefficients 90 volume %	1.0110
k_{10} Frequency factor (s^{-1})	1457.50
k_{20} Frequency factor (s^{-1})	127.59
k_{30} Frequency factor (s^{-1})	1.98
k_{40} Frequency factor (s^{-1})	256.81
k_{50} Frequency factor (s^{-1})	6.29e-4
E_1 Activation Energy (kJ/kg mol)	57,359
E_2 Activation Energy (kJ/kg mol)	52,754
E_3 Activation Energy (kJ/kg mol)	31,820
E_4 Activation Energy (kJ/kg mol)	65,733
E_5 Activation Energy (kJ/kg mol)	66,570
E_c Catalyst Activation Energy (kJ/kg mol)	49,000
ΔH_1 Heat of reaction (kJ/kg)	195
ΔH_2 Heat of reaction (kJ/kg)	670
ΔH_3 Heat of reaction (kJ/kg)	745
ΔH_4 Heat of reaction (kJ/kg)	530
ΔH_5 Heat of reaction (kJ/kg)	690
M_{wH_2} Molecular weights of hydrogen (kg/k mol)	2
M_{wC_1} Molecular weights of methane (kg/k mol)	16
M_{wC_2} Molecular weights of ethane (kg/k mol)	30
M_{wC_3} Molecular weights of propane (kg/k mol)	44
M_{wC_4} Molecular weights of butane (kg/k mol)	58

g, acceleration due to gravity (m/s^2)	9.8
R, ideal gas constant (kPa m3/kg mole K)	8.3143

Acknowledgement:

Petroleum Technology Development Fund, Nigeria, financially sponsored the study.

References:

Ahari, J. S., Farshi, A. and Forsat, K. (2008) A Mathematical Modeling of the Riser Reactor in Industrial FCC Unit. *Petroleum & Coal* 50 (2) 15-24.

Ahmed, T. (2001) *Reservoir Engineering Handbook (2nd Edition).* Elsevier.

Ali, H. and Rohani, S. (1997) Dynamic Modeling and Simulation of a Riser-Type Fluid Catalytic Cracking Unit. *Chemical Engineering Technology* 20 118-130.

Ali, H., Rohani, S. and Corriou, J. P. (1997) Modelling and Control of a Riser Type Fluid Catalytic Cracking (FCC) Unit. *Chemical Engineering Research and Design* 75 (4) 401-412.

Azizi, N., Behbahani, R. and Isazadeh, M. A. (2010) An efficient correlation for calculating compressibility factor of natural gases. *Journal of Natural Gas Chemistry* 19 (6) 642-645.

Bahadori, A., Mokhatab, S. and Towler, B. F. (2007) Rapidly Estimating Natural Gas Compressibility Factor. *Journal of Natural Gas Chemistry* 16 (4) 349-353.

Balachandran, P. (2007) *Fundamentals of Compressible Fluid Dynamics.* New Delhi: Prentice-Hall of India.

Beggs, D. H. and Brill, J. P. (1973) A Study of Two-Phase Flow in Inclined Pipes. *Journal of Petroleum Technology*.

Chang, J., Meng, F., Wang, L., Zhang, K., Chen, H. and Yang, Y. (2012) CFD investigation of hydrodynamics, heat transfer and cracking reaction in a heavy oil riser with bottom airlift loop mixer. *Chemical Engineering Science* 78 128-143.

Chiyoda (1980) *Operating and Unit Manual for the Nigerian National Petroleum Corporation.*

Cristina, P. (2015) Four – Lump Kinetic Model vs. Three - Lump Kinetic Model for the Fluid Catalytic Cracking Riser Reactor. *Procedia Engineering* 100 602-608.

Das, B. S., Saha, R. K. and Gupta, S. P. (2007) Study of Feedstock Injection to Improve Catalyst Homogenization in the Riser of a FCC. *Indian Journal of Chemical Technology* 14 473-480.

Elsharkawy, A. M. (2004) Efficient methods for calculations of compressibility, density and viscosity of natural gases. *Fluid Phase Equilibria* 218 (1) 1-13.

Fayazi, A., Arabloo, M. and Mohammadi, A. H. (2014) Efficient estimation of natural gas compressibility factor using a rigorous method. *Journal of Natural Gas Science and Engineering* 16 8-17.

Fermoselli, N. E. G. (2010) Predicting the Impact of a FCC Turbo Expander on Petroleum Refineries. *Technology* 9 (1) 40-46.

Han, I.-S. and Chung, C.-B. (2001a) Dynamic modeling and simulation of a fluidized catalytic cracking process. Part I: Process modeling. *Chemical Engineering Science* 56 (5) 1951-1971.

Han, I.-S. and Chung, C.-B. (2001b) Dynamic modeling and simulation of a fluidized catalytic cracking process. Part II: Property estimation and simulation. *Chemical Engineering Science* 56 (5) 1973-1990.

He, P., Zhu, C. and Ho, T. C. (2015) A two- zone model for fluid catalytic cracking riser with multiple feed injectors. *AIChE Journal* 61 (2) 610-619.

Heidaryan, E., Moghadasi, J. and Rahimi, M. (2010a) New correlations to predict natural gas viscosity and compressibility factor. *Journal of Petroleum Science and Engineering* 73 (1–2) 67-72.

Heidaryan, E., Salarabadi, A. and Moghadasi, J. (2010b) A novel correlation approach for prediction of natural gas compressibility factor. *Journal of Natural Gas Chemistry* 19 (2) 189-192.

John, Y. M., Patel, R. and Mujtaba, I. M. (2016) Modelling and Simulation of an Industrial Riser in Fluid Catalytic Cracking Process. In Zdravko, K. and Miloš, B. (editors) *Computer Aided Chemical Engineering.* Vol. Volume 38. Elsevier. 889-894.

John, Y. M., Patel, R. and Mujtaba, I. M. (2017a) Maximization of Gasoline in an Industrial Fluidized Catalytic Cracking Unit. *Energy & Fuels*.

John, Y. M., Patel, R. and Mujtaba, I. M. (2017b) Modelling and simulation of an industrial riser in fluid catalytic cracking process. *Computers & Chemical Engineering*.

Kumar, N. (2004) *Compressibility Factors for Natural and Sour Reservoir Gases by Correlations and Cubic Equations of State*. Texas Tech University.

Lee, L.-S., Yu, S.-W. and Cheng, C.-T. (1989) Fluidized-bed Catalyst Cracking Regenerator Modelling and Analysis. *The Chemical Engineering Journal* 40 71-82.

León-Becerril, E., Maya-Yescas, R. and Salazar-Sotelo, D. (2004) Effect of modelling pressure gradient in the simulation of industrial FCC risers. *Chemical Engineering Journal* 100 (1) 181-186.

Li, C., Peng, Y. and Dong, J. (2014) Prediction of compressibility factor for gas condensate under a wide range of pressure conditions based on a three-parameter cubic equation of state. *Journal of Natural Gas Science and Engineering* 20 380-395.

Li, T., Pougatch, K., Salcudean, M. and Grecov, D. (2009) Numerical simulation of single and multiple gas jets in bubbling fluidized beds. *Chemical Engineering Science* 64 (23) 4884-4898.

Liu, L. (2015) *Molecular Characterisation and Modelling for Refining Processes*. Doctor of Philosophy. University of Manchester.

Lopes, G. C., Rosa, L. M., Mori, M., Nunhez, J. R. and Martignoni, W. P. (2012) CFD Study of Industrial FCC Risers: The Effect of Outlet Configurations on Hydrodynamics and Reactions. *International Journal of Chemical Engineering* 2012 1-16.

Mahmoud, M. (2014) Development of a New Correlation of Gas Compressibility Factor (Z-Factor) for High Pressure Gas Reservoirs *Journal of Energy Resources Technology* 136 (1).

Martignoni, W. and de Lasa, H. I. (2001) Heterogeneous reaction model for FCC riser units. *Chemical Engineering Science* 56 (2) 605-612.

Mehran Heydari, H. A. a. B. D. (2010) Study of Seven-Lump Kinetic Model in the Fluid Catalytic Cracking Unit. *American Journal of Applied Sciences 7 (1):* 7 (1) 71-76.

Mujtaba, I. M. (2012) Use of Various Computational Tools and gPROMS for Modelling Simulation Optimisation and Control of Food Processes. In Ahmed, J. and Rahman, M. S. (editors) *Handbook of Food Process Design (1).* Vol. 1. Wiley-Blackwell. 239-261.

Pareek, V. K., Adesina, A. A., Srivastava, A. and Sharma, R. (2003) Modeling of a non-isothermal FCC riser. *Chemical Engineering Journal* 92 (1-3) 101-109.

Pelissari, D. C., Alvarez-Castro, H. C., Mori, M. and Martignoni, W. (2016) Study of Feedstock Injection to Improve Catalyst Homogenization in the Riser of a Fcc. *Brazilian Journal of Chemical Engineering* 33 (3) 559-566.

Pinho, A. d. R., de Almeida, M. B. B., Mendes, F. L., Casavechia, L. C., Talmadge, M. S., Kinchin, C. M. and Chum, H. L. (2017) Fast pyrolysis oil from pinewood chips co-processing with vacuum gas oil in an FCC unit for second generation fuel production. *Fuel* 188 462-473.

Sanjari, E. and Lay, E. N. (2012) Estimation of natural gas compressibility factors using artificial neural network approach. *Journal of Natural Gas Science and Engineering* 9 220-226.

Santos, V. A. d., Dantas, C. C., Luna, C. L., Silva, J. M. F., Lima, A. C., Macieira, R. P. and Verçosa, B. (2007) Simulation of the fluid dynamic parameters in a cold Riser with catalyst density measured by gamma ray Transmission. In *2007 International Nuclear Atlantic Conference - INAC 2007*. Santos, SP, Brazil. ASSOCIAÇÃO BRASILEIRA DE ENERGIA NUCLEAR - ABEN.

Shokir, E. M. E.-M., El-Awad, M. N., Al-Quraishi, A. A. and Al-Mahdy, O. A. (2012) Compressibility factor model of sweet, sour, and condensate gases using genetic programming. *Chemical Engineering Research and Design* 90 (6) 785-792.

Souza, J. A., Vargas, J. V. C., Von Meien, O. F., Martignoni, W. and Amico, S. C. (2006) A two-dimensional model for simulation, control, and optimization of FCC risers. *AIChE Journal* 52 (5) 1895-1905.

Theologos, K. N. and Markatos, N. C. (1993) Advanced modeling of fluid catalytic cracking riser-type reactors. *AIChE Journal* 39 (6) 1007-1017.

Tsuo, Y. P. and Gidaspow, D. (1990) Computation of flow patterns in circulating fluidized beds. *A.I.Ch.E.* 36 885.